

Multi-layer Thermal Analysis for VLSI Chips: A New Technique and Its Mathematical Foundations

Keiji Nakabayashi

Abstract—We present a new technique of multi-layer thermal analysis for VLSI chips. It performs two dimensional, steady-state analysis of thermal conduction and heat generation. Its key component is a new direct method of solving huge systems of linear equations derived from thermal conduction equations. We implemented our technique in C and compared its performance to that of the most effective iterative method of ICCG of LASPAC. Our experimental results demonstrate the superiority of our program by the factors of 3.25 and 6.4 while keeping smaller residuals by 5 and 1 order(s) of magnitude, respectively.

Keywords—thermal analysis, VLSI, Laplace equation, Poisson equation, direct method, ICCG.

I. INTRODUCTION

As semiconductor technology advances in feature size reduction, speed-up, and power reduction, thermal analysis of VLSI chips comes to play more and more important roles in their performances [6][18]. Since the late 1990s, a sizable amount of research activities have been made on the effect of thermal conduction from silicon substrate and heat generated from metal layers on the characteristics of VLSI chips in the post-90 nm era. They are categorized in two major approaches [13].

The first approach starts with a physical equation such as a thermal conduction equation. It then discretizes the equation and solves the generated system of linear equations.

Such a system is then solved by iterative methods such as Incomplete Cholesky Conjugate Gradient (ICCG) method [5] or direct methods such as LU decomposition (LUD) method as well as a special purpose SPICE-like algorithm [1] or a simple tridiagonal band matrix solver, called the Thomas algorithm [14].

In one way, the equation is modeled by finite element method and analyzed by a general purpose solver, called ANSYS through an iterative method or a direct method [4]. Another way uses finite difference method to discretize the equation and analyzes the resultant system of linear equations by a special purpose SPICE-like algorithm [1] or a tridiagonal matrix solver, called the Thomas algorithm in combination with a speed-up technique, called the ADI (Alternative Direction Implicit) method [14].

These methods provide accurate solutions by way of solving thermal equations and are easy to handle different heat sources and a variety of boundary conditions. However, when dealing with large scale thermal analysis for, say an entire chip, the size of the coefficient matrix generated becomes huge and its analysis gets extremely difficult [13].

A new trend of research has recently emerged on thermal analysis for entire VLSI chips with complex shapes and multi-layer structures. This second approach utilizes analogy between heat and electricity to model heat transfer mechanism as RC networks analyzes them using SPICE-like [2][6][17] or a full-chip-scale circuit simulator [1][9].

These methods can be combined with circuit and parasitic analyses and hence it is feasible to realize chip design that takes thermal analysis into consideration. However, the RC networks used become huge and their reduction and approximation are required. As a result, the accuracy of simulation may degrade [13].

It should be noted that a third approach was very recently proposed. It used Green function to describe thermal conduction. However, it cannot be used for transient thermal analysis [15].

We propose a new multi-layer thermal analysis technique along the line of the first approach. It utilizes a new direct method that requires less time and memory than even most iterative methods.

The application of finite difference methods to two or three dimensional Laplace and/or Poisson equations generates large scale systems of linear equations. The coefficient matrices of such systems have a special structure, called block tridiagonal band matrices. Most of the methods and tools thus far proposed use iterative methods for solving the tridiagonal systems of linear equations since such methods require less time and memory than direct methods [4][8][16]. However, the former cannot obtain as accurate solutions as the latter due to an error caused by forced termination of computation [5]. Thus, the direct methods are still preferred in certain situations. Furthermore, in the case of transient thermal analysis, LUD is most often used for easy substitution iteration.

Our technique uses a direct method for block tridiagonal band coefficient matrices. It was derived from a general case linear system solver, called Partial Solution Method (PSM) [12] and is known as Symbolic PSM (S-PSM) in the area of computational fluid dynamics [3]. It was applied to thermal conduction analysis for two and four adjacent materials, where thermal conduction was described by Laplace equations [10].

We demonstrated that S-PSM can be applied to multiple layer materials whose thermal conduction is described by a

K. Nakabayashi is with Integration Technology, Co., Ltd., 2-3-13-105, Minami, Wako, Saitama, Japan (e-mail: nakaba62@gmail.com).

combination of Laplace and Poisson equations [11]. In particular, we consider the case of four layer materials of different thermal conductivities. We then used finite difference method to discretize a combination of Poisson and Laplace equations and generate large scale systems of linear equations. We then applied S-PSM, a block LUD, and ICCG to the linear systems. The experimental results revealed that our method ran 70 times faster, required 3 times less memory, and an order of magnitude smaller residual than LUD. They also showed that the technique achieved up to 3 times speed-up and used 1.8 times smaller memory than ICCG [11].

We improve the technique of [11], and demonstrate that it can solve huge system of linear equations faster. As examples of LSI thermal analysis, we deal with multi-layer interconnect Joule heating problem. We implemented our technique in C and compared its performance to that of the most effective iterative method of ICCG of LSPACK. Our experimental results demonstrate the superiority of our program by the factors of 3.25 and 6.4 while keeping smaller residuals by 5 and 1 order(s) of magnitude, respectively.

In the next section, we provide a complete review of S-PSM using a Poisson equation for the case of a single material. Section III describes a complete review of S-PSM using a set of Poisson equations for the four layer case. Section IV describes a brief overview of its extension to multi-layer case. Section V describes our experiments and compares the results. We conclude the paper in Section VI.

II. S-PSM FOR A SINGLE LAYER

We review an S-PSM solution process as applied to a two-dimensional steady-state thermal conduction analysis of a single material within which heat is generate. Let u denote the material under consideration. Its thermal conduction is modeled by the equation

$$k_u \left(\frac{\partial^2 u}{\partial x^2} + \frac{\partial^2 u}{\partial y^2} \right) = \rho^u \tag{2-1}$$

where variable u denotes the temperature and constants k_u and ρ^u are the thermal conductivity and the heat generation per unit volume of the material u . Note that if heat is not generated from material u , the constant ρ^u on the right hand side of Eq. (2-1) becomes zero and the equation leads to

$$k_u \left(\frac{\partial^2 u}{\partial x^2} + \frac{\partial^2 u}{\partial y^2} \right) = 0 \tag{2-2}$$

When we divide both sides of the above equations (2-1) and (2-2) by the constant k_u , we obtain the Poisson and Laplace equations, respectively. Therefore, we call these equations the Poisson and Laplace thermal conduction equations, respectively, for convenience.

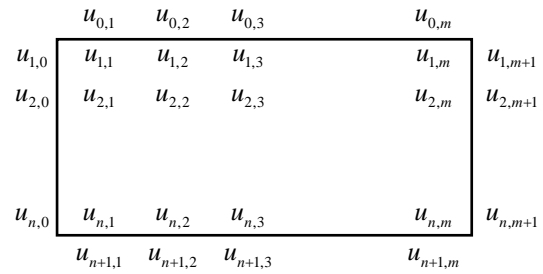


Fig. 2.1: The arrangement of interior grid and boundary points

In order to use the Symbolic Partial Solution Method (S-PSM) to solve Eq. (2-1) numerically we apply finite difference method to discretize it in a certain way. More specifically, we decompose (on) its rectangular domain into $n \times m$ grid points as numbered in Fig. 2.1, where we select the value of n as $n = 2^{\ell+2}$ for some positive integer ℓ .

In the following discussion the indices i and j range as $i = 1, 2, \dots, n$ and $j = 1, 2, \dots, m$. The resulting discretized form of Eq. (2-1) is given as,

$$k_u \left(\frac{u_{i-1,j} - 2u_{i,j} + u_{i+1,j}}{\Delta x^2} + \frac{u_{i,j-1} - 2u_{i,j} + u_{i,j+1}}{\Delta y^2} \right) = \rho_{i,j}^u \tag{2-3}$$

For simplicity we assume that $\Delta x = \Delta y$. The above equation becomes

$$k_u (u_{i-1,j} + u_{i+1,j} + u_{i,j-1} + u_{i,j+1} - 4u_{i,j}) = \Delta x^2 \rho_{i,j}^u \tag{2-4}$$

These equations are combined into the following single matrix-vector form such that the matrix of order n has tridiagonal elements of blocks.

$$\begin{pmatrix} A_1^{(0)} & k_u I & O \\ k_u I & A_1^{(0)} & k_u I & O \\ O & k_u I & A_1^{(0)} & k_u I & O \\ & & & \bullet \\ & & & & \bullet \\ & & & & & \bullet \\ & & & & & & \bullet \\ & & & & & & & \bullet \\ & & & & & & & & O & k_u I & A_1^{(0)} & k_u I \\ & & & & & & & & & O & k_u I & A_1^{(0)} \end{pmatrix} \begin{pmatrix} \mathbf{u}_1^{(0)} \\ \mathbf{u}_2^{(0)} \\ \mathbf{u}_3^{(0)} \\ \bullet \\ \bullet \\ \bullet \\ \bullet \\ \bullet \\ \mathbf{u}_{n-1}^{(0)} \\ \mathbf{u}_n^{(0)} \end{pmatrix} = \begin{pmatrix} \mathbf{f}_{u,1}^{(0)} \\ \mathbf{f}_{u,2}^{(0)} \\ \mathbf{f}_{u,3}^{(0)} \\ \bullet \\ \bullet \\ \bullet \\ \bullet \\ \mathbf{f}_{u,n-1}^{(0)} \\ \mathbf{f}_{u,n}^{(0)} \end{pmatrix} - \begin{pmatrix} k_u \mathbf{u}_0^{(0)} \\ \mathbf{0} \\ \mathbf{0} \\ \bullet \\ \bullet \\ \bullet \\ \mathbf{0} \\ \mathbf{0} \\ k_u \mathbf{u}_{n+1}^{(0)} \end{pmatrix} \tag{2-5}$$

where O is a zero matrix of order m , I is a unit matrix of order m , $\mathbf{0}$ is a zero column vector of order m , and matrix $A_1^{(0)}$ and column vectors $\mathbf{u}_i^{(0)}$ and $\mathbf{f}_{u,i}^{(0)}$ of order m each are given by

$$A_1^{(0)} = \begin{pmatrix} -4k_u & k_u & 0 & & & \\ k_u & -4k_u & k_u & 0 & & \\ 0 & k_u & -4k_u & k_u & 0 & \\ & & & \ddots & & \\ & & & & 0 & k_u & -4k_u & k_u \\ & & & & & & 0 & k_u & -4k_u \end{pmatrix} \quad (2-6)$$

$$\mathbf{u}_i^{(0)} = (u_{i,1} \quad u_{i,2} \quad u_{i,3} \quad \dots \quad u_{i,m-1} \quad u_{i,m})^T \quad (2-7)$$

$$\mathbf{u}_0^{(0)} = (u_{0,1} \quad u_{0,2} \quad u_{0,3} \quad \dots \quad u_{0,m-1} \quad u_{0,m})^T \quad (2-8)$$

$$\mathbf{u}_{n+1}^{(0)} = (u_{n+1,1} \quad u_{n+1,2} \quad u_{n+1,3} \quad \dots \quad u_{n+1,m-1} \quad u_{n+1,m})^T \quad (2-9)$$

$$\mathbf{f}_{u,i}^{(0)} = (-k_u u_{i,0} + \Delta x^2 \rho_{i,1}^u \quad \Delta x^2 \rho_{i,2}^u \quad \dots \quad \Delta x^2 \rho_{i,m-1}^u \quad -k_u u_{i,m+1} + \Delta x^2 \rho_{i,m}^u)^T \quad (2-10)$$

Note that the vector $\mathbf{f}_{u,i}^{(0)}$ represents the boundary conditions.

The discretized form of the Laplace thermal conduction equation expressed of Eq. (2-2) is obtained by setting variables $\rho_{i,j}$ to zero in Eq. (2-10). In other words, Eq. (2-10) becomes

$$\mathbf{f}_{u,i}^{(0)} = (-k_u u_{i,0} \quad 0 \quad 0 \quad \dots \quad 0 \quad -k_u u_{i,m+1})^T \quad (2-11)$$

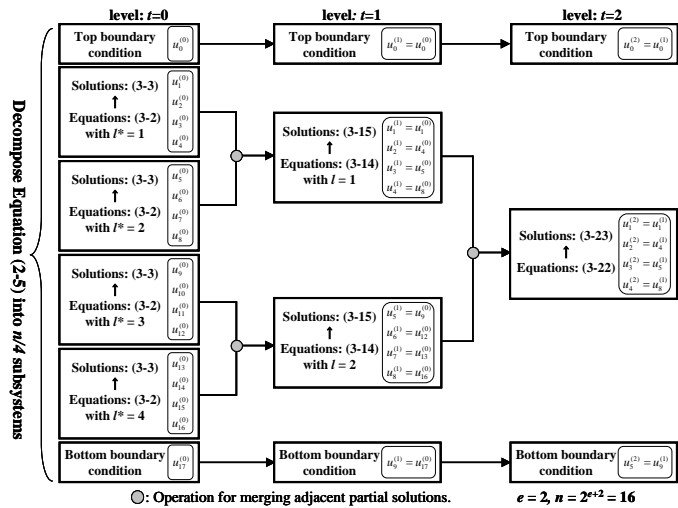


Fig. 2.2: An overall computation flow with relevant equation numbers of a S-PSM-based solution process of a Poisson thermal conduction equation.

To solve Eq. (2-5), we first partition the tridiagonal band part of its coefficient matrix into $n/4$ submatrices. As $n = 2^{e+2}$ each of the resultant submatrices is a 4×4 matrix. We say that these submatrices and their corresponding subsystems of equations are at the 0-th level. The l^* -th subsystem, with $l^* = 1, 2, \dots, n/4$, at the 0-th level is given by

$$\begin{pmatrix} A_1^{(0)} & k_u I & O & O \\ k_u I & A_1^{(0)} & k_u I & O \\ O & k_u I & A_1^{(0)} & k_u I \\ O & O & k_u I & A_1^{(0)} \end{pmatrix} \begin{pmatrix} \mathbf{u}_{4(l^*-1)+1}^{(0)} \\ \mathbf{u}_{4(l^*-1)+2}^{(0)} \\ \mathbf{u}_{4(l^*-1)+3}^{(0)} \\ \mathbf{u}_{4l^*}^{(0)} \end{pmatrix} = \begin{pmatrix} \mathbf{f}_{u,4(l^*-1)+1}^{(0)} \\ \mathbf{f}_{u,4(l^*-1)+2}^{(0)} \\ \mathbf{f}_{u,4(l^*-1)+3}^{(0)} \\ \mathbf{f}_{u,4l^*}^{(0)} \end{pmatrix} - \begin{pmatrix} k_u \mathbf{u}_{4(l^*-1)}^{(0)} \\ \mathbf{0} \\ \mathbf{0} \\ k_u \mathbf{u}_{4l^*+1}^{(0)} \end{pmatrix} \quad (2-12)$$

The solution of the above equation is given by

$$\begin{pmatrix} \mathbf{u}_{4(l^*-1)+1}^{(0)} \\ \mathbf{u}_{4(l^*-1)+2}^{(0)} \\ \mathbf{u}_{4(l^*-1)+3}^{(0)} \\ \mathbf{u}_{4l^*}^{(0)} \end{pmatrix} = T_{(l^*)}^{(0)-1} \begin{pmatrix} \mathbf{f}_{u,4(l^*-1)+1}^{(0)} \\ \mathbf{f}_{u,4(l^*-1)+2}^{(0)} \\ \mathbf{f}_{u,4(l^*-1)+3}^{(0)} \\ \mathbf{f}_{u,4l^*}^{(0)} \end{pmatrix} - \begin{pmatrix} k_u \mathbf{u}_{4(l^*-1)}^{(0)} \\ \mathbf{0} \\ \mathbf{0} \\ k_u \mathbf{u}_{4l^*+1}^{(0)} \end{pmatrix} \quad (2-13)$$

where

$$T_{(l^*)}^{(0)-1} = \begin{pmatrix} A_1^{(0)} & k_u I & O & O \\ k_u I & A_1^{(0)} & k_u I & O \\ O & k_u I & A_1^{(0)} & k_u I \\ O & O & k_u I & A_1^{(0)} \end{pmatrix}^{-1} = \begin{pmatrix} B_1^{(0)} & B_2^{(0)} & B_3^{(0)} & B_4^{(0)} \\ B_2^{(0)} & B_5^{(0)} & B_6^{(0)} & B_3^{(0)} \\ B_3^{(0)} & B_6^{(0)} & B_5^{(0)} & B_2^{(0)} \\ B_4^{(0)} & B_3^{(0)} & B_2^{(0)} & B_1^{(0)} \end{pmatrix} \quad (2-14)$$

and

$$\left. \begin{aligned} C &= \left(\frac{1}{k_u}\right) A_1^{(0)}, \quad D = \left(\frac{1}{k_u}\right) [C - I]^2 - [C]^2 \\ B_1^{(0)} &= CD((C)^2 - I), \quad B_2^{(0)} = -D((C)^2 - I) \\ B_3^{(0)} &= CD, \quad B_4^{(0)} = -D, \quad B_5^{(0)} = CD((C)^2 - I), \quad B_6^{(0)} = -D(C)^2 \end{aligned} \right\} \quad (2-15)$$

As depicted in Fig. 2.2 and explained below, the next step of the S-PSM-based solution process is to work on pairs of the above subsystems. We will merge a pair of subsystems at the $(t-1)$ st level to obtain a subsystem at the t -th level, where $t = 1, 2, \dots, e-1$. Note that solutions for the middle two column vectors of variables of each subsystem are readily available. Therefore, the remaining first and fourth vectors of variables of the l -th subsystem, with $l = 1, 2, \dots, n/2^{t+1}$, at the 0-th level are renamed as the first and second vectors at the 1st level as follows.

$$\left. \begin{aligned} \mathbf{u}_{2l-1}^{(1)} &= \mathbf{u}_{4(l-1)+1}^{(0)} \\ \mathbf{u}_{2l}^{(1)} &= \mathbf{u}_{4l}^{(0)} \end{aligned} \right\} \quad (2-16)$$

From Eq. (2-13) the right hand side of the above equations are expressed by

$$\left. \begin{aligned} \mathbf{u}_{4(l-1)+1}^{(0)} &= -A_1^{(1)} \mathbf{u}_{4(l-1)}^{(0)} - A_2^{(1)} \mathbf{u}_{4l+1}^{(0)} + \mathbf{f}_{u,2l-1}^{(1)} \\ \mathbf{u}_{4l}^{(0)} &= -A_2^{(1)} \mathbf{u}_{4(l-1)}^{(0)} - A_1^{(1)} \mathbf{u}_{4l+1}^{(0)} + \mathbf{f}_{u,2l}^{(1)} \end{aligned} \right\} \quad (2-17)$$

where

$$A_1^{(1)} \equiv k_u B_1^{(0)}, \quad A_2^{(1)} \equiv k_u B_4^{(0)} \quad (2-18)$$

$$\left. \begin{aligned} \mathbf{f}_{u,2l-1}^{(1)} &= B_1^{(0)} \mathbf{f}_{u,4(l-1)+1}^{(0)} + B_2^{(0)} \mathbf{f}_{u,4(l-1)+2}^{(0)} + B_3^{(0)} \mathbf{f}_{u,4(l-1)+3}^{(0)} + B_4^{(0)} \mathbf{f}_{u,4l}^{(0)} \\ \mathbf{f}_{u,2l}^{(1)} &= B_4^{(0)} \mathbf{f}_{u,4(l-1)+1}^{(0)} + B_3^{(0)} \mathbf{f}_{u,4(l-1)+2}^{(0)} + B_2^{(0)} \mathbf{f}_{u,4(l-1)+3}^{(0)} + B_1^{(0)} \mathbf{f}_{u,4l}^{(0)} \end{aligned} \right\} \quad (2-19)$$

Using Eq. (2-16), Eq. (2-17) is rewritten as

$$\left. \begin{aligned} \mathbf{u}_{2l-1}^{(1)} &= -A_1^{(1)} \mathbf{u}_{2l-2}^{(1)} - A_2^{(1)} \mathbf{u}_{2l+1}^{(1)} + \mathbf{f}_{u,2l-1}^{(1)} \\ \mathbf{u}_{2l}^{(1)} &= -A_2^{(1)} \mathbf{u}_{2l-2}^{(1)} - A_1^{(1)} \mathbf{u}_{2l+1}^{(1)} + \mathbf{f}_{u,2l}^{(1)} \end{aligned} \right\} \quad (2-20)$$

Similarly, the $(l+1)$ st subsystem is expressed as

$$\left. \begin{aligned} \mathbf{u}_{2l+1}^{(1)} &= -A_1^{(1)} \mathbf{u}_{2l}^{(1)} - A_2^{(1)} \mathbf{u}_{2l+3}^{(1)} + \mathbf{f}_{u,2l+1}^{(1)} \\ \mathbf{u}_{2l+2}^{(1)} &= -A_2^{(1)} \mathbf{u}_{2l}^{(1)} - A_1^{(1)} \mathbf{u}_{2l+3}^{(1)} + \mathbf{f}_{u,2l+2}^{(1)} \end{aligned} \right\} \quad (2-21)$$

Combining (2-20) and (2-21), we have

$$\begin{pmatrix} I & 0 & A_2^{(1)} & 0 \\ 0 & I & A_1^{(1)} & 0 \\ 0 & A_1^{(1)} & I & 0 \\ 0 & A_2^{(1)} & 0 & I \end{pmatrix} \begin{pmatrix} \mathbf{u}_{2l-1}^{(1)} \\ \mathbf{u}_{2l}^{(1)} \\ \mathbf{u}_{2l+1}^{(1)} \\ \mathbf{u}_{2l+2}^{(1)} \end{pmatrix} = \begin{pmatrix} \mathbf{f}_{u,2l-1}^{(1)} \\ \mathbf{f}_{u,2l}^{(1)} \\ \mathbf{f}_{u,2l+1}^{(1)} \\ \mathbf{f}_{u,2l+2}^{(1)} \end{pmatrix} - \begin{pmatrix} A_1^{(1)}\mathbf{u}_{2l-2}^{(1)} \\ A_2^{(1)}\mathbf{u}_{2l-2}^{(1)} \\ A_2^{(1)}\mathbf{u}_{2l+3}^{(1)} \\ A_1^{(1)}\mathbf{u}_{2l+3}^{(1)} \end{pmatrix} \quad (2-22)$$

Upon re-indexing the vectors, the above equation becomes

$$\begin{pmatrix} I & 0 & A_2^{(1)} & 0 \\ 0 & I & A_1^{(1)} & 0 \\ 0 & A_1^{(1)} & I & 0 \\ 0 & A_2^{(1)} & 0 & I \end{pmatrix} \begin{pmatrix} \mathbf{u}_{4(l-1)+1}^{(1)} \\ \mathbf{u}_{4(l-1)+2}^{(1)} \\ \mathbf{u}_{4(l-1)+3}^{(1)} \\ \mathbf{u}_{4l}^{(1)} \end{pmatrix} = \begin{pmatrix} \mathbf{f}_{u,4(l-1)+1}^{(1)} \\ \mathbf{f}_{u,4(l-1)+2}^{(1)} \\ \mathbf{f}_{u,4(l-1)+3}^{(1)} \\ \mathbf{f}_{u,4l}^{(1)} \end{pmatrix} - \begin{pmatrix} A_1^{(1)}\mathbf{u}_{4(l-1)}^{(1)} \\ A_2^{(1)}\mathbf{u}_{4(l-1)}^{(1)} \\ A_2^{(1)}\mathbf{u}_{4l+1}^{(1)} \\ A_1^{(1)}\mathbf{u}_{4l+1}^{(1)} \end{pmatrix} \quad (2-23)$$

In general, after merging a pair of subsystems at the $(t-1)$ st level, we obtain a subsystem at the t -th level as shown below. Note that $t = 1, 2, \dots, e-1$.

$$\begin{pmatrix} I & 0 & A_2^{(t)} & 0 \\ 0 & I & A_1^{(t)} & 0 \\ 0 & A_1^{(t)} & I & 0 \\ 0 & A_2^{(t)} & 0 & I \end{pmatrix} \begin{pmatrix} \mathbf{u}_{4(l-1)+1}^{(t)} \\ \mathbf{u}_{4(l-1)+2}^{(t)} \\ \mathbf{u}_{4(l-1)+3}^{(t)} \\ \mathbf{u}_{4l}^{(t)} \end{pmatrix} = \begin{pmatrix} \mathbf{f}_{u,4(l-1)+1}^{(t)} \\ \mathbf{f}_{u,4(l-1)+2}^{(t)} \\ \mathbf{f}_{u,4(l-1)+3}^{(t)} \\ \mathbf{f}_{u,4l}^{(t)} \end{pmatrix} - \begin{pmatrix} A_1^{(t)}\mathbf{u}_{4(l-1)}^{(t)} \\ A_2^{(t)}\mathbf{u}_{4(l-1)}^{(t)} \\ A_2^{(t)}\mathbf{u}_{4l+1}^{(t)} \\ A_1^{(t)}\mathbf{u}_{4l+1}^{(t)} \end{pmatrix} \quad (2-24)$$

The solution of the above equation is given by

$$\begin{pmatrix} \mathbf{u}_{4(l-1)+1}^{(t)} \\ \mathbf{u}_{4(l-1)+2}^{(t)} \\ \mathbf{u}_{4(l-1)+3}^{(t)} \\ \mathbf{u}_{4l}^{(t)} \end{pmatrix} = T_{(l)}^{(t)-1} \left(\begin{pmatrix} \mathbf{f}_{u,4(l-1)+1}^{(t)} \\ \mathbf{f}_{u,4(l-1)+2}^{(t)} \\ \mathbf{f}_{u,4(l-1)+3}^{(t)} \\ \mathbf{f}_{u,4l}^{(t)} \end{pmatrix} - \begin{pmatrix} A_1^{(t)}\mathbf{u}_{4(l-1)}^{(t)} \\ A_2^{(t)}\mathbf{u}_{4(l-1)}^{(t)} \\ A_2^{(t)}\mathbf{u}_{4l+1}^{(t)} \\ A_1^{(t)}\mathbf{u}_{4l+1}^{(t)} \end{pmatrix} \right) \quad (2-25)$$

where

$$T_{(l)}^{(t)-1} = \begin{pmatrix} I & O & A_2^{(t)} & O \\ O & I & A_1^{(t)} & O \\ O & A_1^{(t)} & I & O \\ O & A_2^{(t)} & O & I \end{pmatrix}^{-1} = \begin{pmatrix} I & B_1^{(t)} & B_4^{(t)} & O \\ O & B_2^{(t)} & B_3^{(t)} & O \\ O & B_3^{(t)} & B_2^{(t)} & O \\ O & B_4^{(t)} & B_1^{(t)} & I \end{pmatrix} \quad (2-26)$$

and

$$\left. \begin{aligned} B_1^{(t)} &= -A_2^{(t)}A_1^{(t)}((A_1^{(t)})^2 - I)^{-1}, & B_2^{(t)} &= -((A_1^{(t)})^2 - I)^{-1} \\ B_3^{(t)} &= A_1^{(t)}((A_1^{(t)})^2 - I)^{-1}, & B_4^{(t)} &= A_2^{(t)}((A_1^{(t)})^2 - I)^{-1} \end{aligned} \right\} \quad (2-27)$$

As seen from the right hand side of Eq. (2-25), the solutions for the four vectors on the left hand side are obtained once we solve for the two vectors on the right hand side, which are the fourth vector of the $(l-1)$ st subsystem and the first vector of the $(l+1)$ st subsystem both at the t -th level, where $l = 1, 2, \dots, n/2^{t+2}$. Therefore, we re-index the vectors as shown below and merge the pair of the l -th and $(l+1)$ st subsystems at the t -th level to obtain the $(t+1)$ st level subsystem of two equations

$$\left. \begin{aligned} \mathbf{u}_{2l-1}^{(t+1)} &= \mathbf{u}_{4(l-1)+1}^{(t)} \\ \mathbf{u}_{2l}^{(t+1)} &= \mathbf{u}_{4l}^{(t)} \end{aligned} \right\} \quad (2-28)$$

where

$$A_1^{(t+1)} \equiv A_1^{(t)} + B_1^{(t)}A_2^{(t)}, \quad A_2^{(t+1)} \equiv B_4^{(t)}A_2^{(t)} \quad (2-29)$$

$$\left. \begin{aligned} \mathbf{u}_{2l-1}^{(t+1)} &= -A_1^{(t+1)}\mathbf{u}_{2l-2}^{(t+1)} - A_2^{(t+1)}\mathbf{u}_{2l+1}^{(t+1)} + \mathbf{f}_{u,2l-1}^{(t+1)} \\ \mathbf{u}_{2l}^{(t+1)} &= -A_2^{(t+1)}\mathbf{u}_{2l-2}^{(t+1)} - A_1^{(t+1)}\mathbf{u}_{2l+1}^{(t+1)} + \mathbf{f}_{u,2l}^{(t+1)} \end{aligned} \right\} \quad (2-30)$$

$$\left. \begin{aligned} \mathbf{f}_{u,2l-1}^{(t+1)} &= \mathbf{f}_{u,4(l-1)+1}^{(t)} + B_1^{(t)}\mathbf{f}_{u,4(l-1)+2}^{(t)} + B_4^{(t)}\mathbf{f}_{u,4(l-1)+3}^{(t)} \\ \mathbf{f}_{u,2l}^{(t+1)} &= B_4^{(t)}\mathbf{f}_{u,4(l-1)+2}^{(t)} + B_1^{(t)}\mathbf{f}_{u,4(l-1)+3}^{(t)} + \mathbf{f}_{u,4l}^{(t)} \end{aligned} \right\} \quad (2-31)$$

At the end of the above merging process, we have the following single subsystem of four equations at e -th level.

$$\begin{pmatrix} I & 0 & A_2^{(e)} & 0 \\ 0 & I & A_1^{(e)} & 0 \\ 0 & A_1^{(e)} & I & 0 \\ 0 & A_2^{(e)} & 0 & I \end{pmatrix} \begin{pmatrix} \mathbf{u}_1^{(e)} \\ \mathbf{u}_2^{(e)} \\ \mathbf{u}_3^{(e)} \\ \mathbf{u}_4^{(e)} \end{pmatrix} = \begin{pmatrix} \mathbf{f}_{u,1}^{(e)} \\ \mathbf{f}_{u,2}^{(e)} \\ \mathbf{f}_{u,3}^{(e)} \\ \mathbf{f}_{u,4}^{(e)} \end{pmatrix} - \begin{pmatrix} A_1^{(e)}\mathbf{u}_0^{(e)} \\ A_2^{(e)}\mathbf{u}_5^{(e)} \\ A_2^{(e)}\mathbf{u}_5^{(e)} \\ A_1^{(e)}\mathbf{u}_5^{(e)} \end{pmatrix} \quad (2-32)$$

The solution of the above equation is given by

$$\begin{pmatrix} \mathbf{u}_1^{(e)} \\ \mathbf{u}_2^{(e)} \\ \mathbf{u}_3^{(e)} \\ \mathbf{u}_4^{(e)} \end{pmatrix} = T_{(1)}^{(e)-1} \left(\begin{pmatrix} \mathbf{f}_{u,1}^{(e)} \\ \mathbf{f}_{u,2}^{(e)} \\ \mathbf{f}_{u,3}^{(e)} \\ \mathbf{f}_{u,4}^{(e)} \end{pmatrix} - \begin{pmatrix} A_1^{(e)}\mathbf{u}_0^{(e)} \\ A_2^{(e)}\mathbf{u}_5^{(e)} \\ A_2^{(e)}\mathbf{u}_5^{(e)} \\ A_1^{(e)}\mathbf{u}_5^{(e)} \end{pmatrix} \right) \quad (2-33)$$

where

$$T_{(1)}^{(e)-1} = \begin{pmatrix} I & O & A_2^{(e)} & O \\ O & I & A_1^{(e)} & O \\ O & A_1^{(e)} & I & O \\ O & A_2^{(e)} & O & I \end{pmatrix}^{-1} = \begin{pmatrix} I & B_1^{(e)} & B_4^{(e)} & O \\ O & B_2^{(e)} & B_3^{(e)} & O \\ O & B_3^{(e)} & B_2^{(e)} & O \\ O & B_4^{(e)} & B_1^{(e)} & I \end{pmatrix} \quad (2-34)$$

and

$$\left. \begin{aligned} B_1^{(e)} &= -A_2^{(e)}A_1^{(e)}((A_1^{(e)})^2 - I)^{-1}, & B_2^{(e)} &= -((A_1^{(e)})^2 - I)^{-1} \\ B_3^{(e)} &= A_1^{(e)}((A_1^{(e)})^2 - I)^{-1}, & B_4^{(e)} &= A_2^{(e)}((A_1^{(e)})^2 - I)^{-1} \end{aligned} \right\} \quad (2-35)$$

Note that in the above process of merging, we need to consider the four boundary conditions. The upper boundary value stays the same at any level. The lower one gets a new index given by $n/2^{t+1}+1$ at the $(t+1)$ st level. More precisely,

$$\left. \begin{aligned} \mathbf{u}_0^{(t+1)} &= \mathbf{u}_0^{(0)} \\ \mathbf{u}_{n/2^{t+1}+1}^{(t+1)} &= \mathbf{u}_{n+1}^{(0)} \end{aligned} \right\} \quad (2-36)$$

In order to have a clearer view of understanding the merging of two adjacent materials at their boundary, we rewrite Eq. (2-33) as follows:

$$\left. \begin{aligned} \mathbf{u}_1^{(e)} &= \mathbf{f}_{u,1}^{(e)} + B_1^{(e)}\mathbf{f}_{u,2}^{(e)} + B_4^{(e)}\mathbf{f}_{u,3}^{(e)} - (A_1^{(e)} + B_1^{(e)}A_2^{(e)})\mathbf{u}_0^{(e)} - B_4^{(e)}A_2^{(e)}\mathbf{u}_5^{(e)} \\ \mathbf{u}_2^{(e)} &= B_2^{(e)}\mathbf{f}_{u,2}^{(e)} + B_3^{(e)}\mathbf{f}_{u,3}^{(e)} - B_2^{(e)}A_2^{(e)}\mathbf{u}_0^{(e)} - B_3^{(e)}A_2^{(e)}\mathbf{u}_5^{(e)} \\ \mathbf{u}_3^{(e)} &= B_3^{(e)}\mathbf{f}_{u,2}^{(e)} + B_2^{(e)}\mathbf{f}_{u,3}^{(e)} - B_3^{(e)}A_2^{(e)}\mathbf{u}_0^{(e)} - B_2^{(e)}A_2^{(e)}\mathbf{u}_5^{(e)} \\ \mathbf{u}_4^{(e)} &= B_4^{(e)}\mathbf{f}_{u,2}^{(e)} + B_1^{(e)}\mathbf{f}_{u,3}^{(e)} + \mathbf{f}_{u,4}^{(e)} - B_4^{(e)}A_2^{(e)}\mathbf{u}_0^{(e)} - (A_1^{(e)} + B_1^{(e)}A_2^{(e)})\mathbf{u}_5^{(e)} \end{aligned} \right\} \quad (2-37)$$

Using the relations,

$$A_1^{(e+1)} \equiv A_1^{(e)} + B_1^{(e)}A_2^{(e)}, \quad A_2^{(e+1)} \equiv B_4^{(e)}A_2^{(e)} \quad (2-38)$$

the first and fourth equations of (2-37) are expressed as

$$\left. \begin{aligned} \mathbf{u}_1^{(e)} &= \mathbf{f}_{u,1}^{(e+1)} - A_1^{(e+1)}\mathbf{u}_0^{(e)} - A_2^{(e+1)}\mathbf{u}_5^{(e)} \\ \mathbf{u}_4^{(e)} &= \mathbf{f}_{u,2}^{(e+1)} - A_2^{(e+1)}\mathbf{u}_0^{(e)} - A_1^{(e+1)}\mathbf{u}_5^{(e)} \end{aligned} \right\} \quad (2-39)$$

As the values for the vectors $\mathbf{u}_0^{(e)}$ and $\mathbf{u}_5^{(e)}$ are given, we get the solutions for $\mathbf{u}_1^{(e)}$ and $\mathbf{u}_4^{(e)}$. Substituting these values into Eq. (2-37), we find the solutions for $\mathbf{u}_2^{(e)}$ and $\mathbf{u}_3^{(e)}$.

Starting with those values with the aid of the following relations expressed as Eq. (2-40), we can solve the subsystems at the t -th level from those at the $(t+1)$ st level for $t = e-1, e-2, \dots, 1$, as depicted in Fig. 2.3.

$$\left. \begin{aligned} \mathbf{u}_{4(l^*-1)+2}^{(t)} &= B_2^{(t)} \mathbf{f}_{u,4(l^*-1)+2}^{(t)} + B_3^{(t)} \mathbf{f}_{u,4(l^*-1)+3}^{(t)} - B_2^{(t)} A_2^{(t)} \mathbf{u}_{4(l^*-1)}^{(t)} - B_3^{(t)} A_2^{(t)} \mathbf{u}_{4l^*+1}^{(t)} \\ \mathbf{u}_{4(l^*-1)+3}^{(t)} &= B_3^{(t)} \mathbf{f}_{u,4(l^*-1)+2}^{(t)} + B_2^{(t)} \mathbf{f}_{u,4(l^*-1)+3}^{(t)} - B_3^{(t)} A_2^{(t)} \mathbf{u}_{4(l^*-1)}^{(t)} - B_2^{(t)} A_2^{(t)} \mathbf{u}_{4l^*+1}^{(t)} \end{aligned} \right\} \quad (2-40)$$

$$(l^* = n/2^{t+2}, \dots, 2, 1)$$

At the last step, we get the solutions for the remaining vectors as follows:

$$\left. \begin{aligned} \mathbf{u}_{4(l^*-1)+2}^{(0)} &= B_2^{(0)} \mathbf{f}_{u,4(l^*-1)+2}^{(0)} + B_5^{(0)} \mathbf{f}_{u,4(l^*-1)+2}^{(0)} + B_6^{(0)} \mathbf{f}_{u,4(l^*-1)+3}^{(0)} + B_3^{(0)} \mathbf{f}_{u,4l^*}^{(0)} \\ &\quad - k_u B_2^{(0)} \mathbf{u}_{4(l^*-1)}^{(0)} - k_u B_3^{(0)} \mathbf{u}_{4l^*+1}^{(0)} \\ \mathbf{u}_{4(l^*-1)+3}^{(0)} &= B_3^{(0)} \mathbf{f}_{u,4(l^*-1)+2}^{(0)} + B_6^{(0)} \mathbf{f}_{u,4(l^*-1)+2}^{(0)} + B_5^{(0)} \mathbf{f}_{u,4(l^*-1)+3}^{(0)} + B_2^{(0)} \mathbf{f}_{u,4l^*}^{(0)} \\ &\quad - k_u B_3^{(0)} \mathbf{u}_{4(l^*-1)}^{(0)} - k_u B_2^{(0)} \mathbf{u}_{4l^*+1}^{(0)} \end{aligned} \right\} \quad (2-41)$$

$$(l^* = 1, 2, \dots, n/4)$$

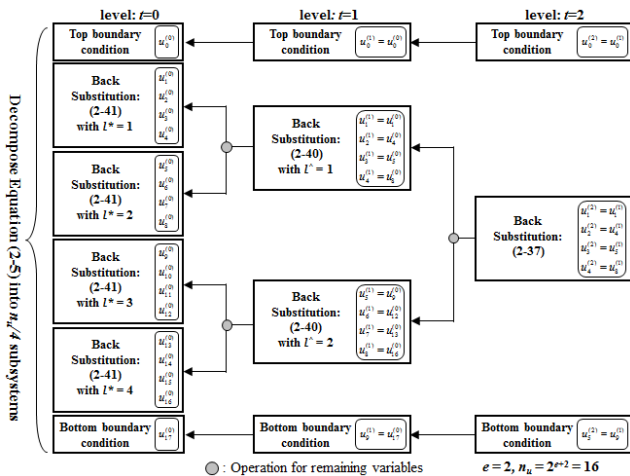


Fig. 2.3: An overall computation flow with relevant equation numbers of an S-PSM-based back substitution process of a Poisson thermal conduction equation.

III. S-PSM FOR FOUR LAYERS

We consider a thermal analysis using a basic structural pattern of a VLSI chip consisting of four layer materials. Thermal conduction of some materials within which heat is generated is expressed by a set of Poisson equations. Thermal conduction of other materials within which heat is not generated is expressed by a set of Laplace equations. The Laplace equation is a special case of Poisson equation in that its right hand side is equal to zero. Therefore, in generalized, thermal conduction of the

multi-layer material structure can be expressed as a set of Poisson equations. For materials within which heat is not generated, the right hand side of its Poisson equation is set to zero. In this chapter, we consider a set of Poisson equations corresponding to four layers of materials. We apply an S-PSM-based solution method which was discussed in the Chapter 2 to solve four Poisson thermal conduction equations at a time.

In the next section, we explain how S-PSM works using our four layer example.

3.1 The Problem

We consider a multi-layer structure as depicted in Fig. 3.1, where four layers of materials $p, q, r,$ and s of thermal conductivities $k_p, k_q, k_r,$ and $k_s,$ respectively, are stacked together. This structure may represent a basic pattern of a VLSI chip, where the layers are from the bottom, SiO₂, Cu (copper wire), ILD (interlayer dielectric), and passivation. Heat is generated due to Joule heating only from the copper wire. The heat travels through a heat transfer pass consisting of the Cu, ILD, and passivation, and goes out to the ambient air. Our problem is to find temperature distribution through two-dimensional steady-state thermal conduction analysis.

In this multi-layer structure, the materials $p, q, r,$ and s correspond to the passivation, ILD, Cu, and SiO₂, respectively. Because heat is generated from Cu, the thermal conduction of material r is described by a Poisson thermal conduction equation of Eq. (2-1). Because the other materials SiO₂, ILD, and passivation do not generate heat, the thermal conduction of materials $p, q,$ and s is described by a Poisson thermal conduction equation whose right hand side is set to zero.

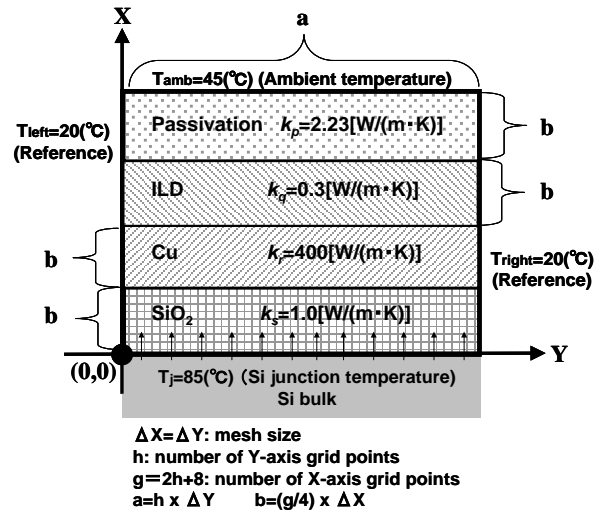


Fig. 3.1: Two dimensional analysis for steady-state heat conduction of four materials of thermal conductivities $k_p, k_q, k_r,$ and $k_s.$

3.2 S-PSM-based Solution Process

We describe the concept and a computational procedure of the linear equation solver, called S-PSM as applied to Poisson

thermal conduction equations. Given a system of linear equations derived by FDM, the S-PSM decomposes it into its subsystems and finds the values of the variables shared by each pair of adjacent subsystems. Figure 3.2 shows an overall flow of the major algebraic computations to take place at each subsystem with their relevant equations and solutions specified.

It should be noted from the figure that the S-PSM-based solution process goes through many levels of repeated operations of decomposition and merging. In the following section, the level information is attached to variable vectors and coefficient submatrices as their superscripts with parentheses such as (0) and (e).

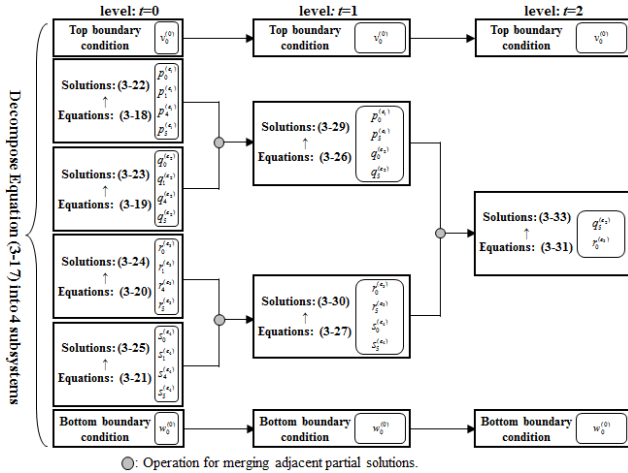


Fig. 3.2: An overall computation flow with relevant equation numbers of a S-PSM-based solution process of Poisson thermal conduction thermal equations for four materials.

3.2.1 Poisson Thermal Conduction and Finite Difference Equations

The thermal conduction is described by the Poisson thermal conduction equation. The thermal conduction of the four materials *p*, *q*, *r* and *s* are described by a Poisson thermal conduction equation that is expressed as Eq. (2-1).

In our analysis, the bold lower case letter *u* represents one of the four materials *p*, *q*, *r* and *s* and the lower case letter *u* denotes one of their corresponding variable names *p*, *q*, *r* and *s*. So we have a set of four Poisson thermal conduction equations to solve.

When we apply FDM to Eq. (2-1), we decompose each of the corresponding rectangle domains into a grid of $(n_u+2) \times m$ points to which variables are assigned as shown inside each rectangle of Fig. 3.3. Note that there are (n_u+2) rows of grid points instead of n_u . It is unlike the single material case as depicted in Fig. 2.1 of the Chapter 2. As discussed in section 3.2.2, we need a single extra row of grid of *m* points respectively, at the top and bottom borders of each of the rectangle domains so as to define the equivalent thermal conductivity of the connection boundary between adjacent materials. In other words, the grid of $n_u \times m$ points in each material is used to obtain a solution for each material, as discussed in the Chapter 2. In addition, the grid of *m*

points, which are set at the top and the bottom borders of each material, is used to connect adjacent materials.

For the sake of simplicity, we make two assumptions:

- (1) Each cell of the four grids is a square of the same size, that is, $\Delta x = \Delta y$.
- (2) The number of X-axis grid points for each material *u* (*p*, *q*, *r*, *s*) is a power of 2, that is,

$$n_p = 2^{e_1+2}, n_q = 2^{e_2+2}, n_r = 2^{e_3+2}, n_s = 2^{e_4+2} \quad (3-1)$$

for some positive integers e_1, e_2, e_3 and e_4 , respectively.

We apply finite difference method (FDM) on its rectangular domain of grid points in each material of Fig. 3.3 and discretize Eq. (2-1). The resulting discretized form of Eq. (2-1) is given as Eq. (2-4). These equations are combined into the single matrix-vector form and are expressed as Eq. (2-5). Then, the boundary condition is expressed as Eq. (2-10). This system of linear equation is solved in each material.

3.2.2 Boundary Conditions

As shown in Fig. 3.1, the upper and lower boundary conditions are the ambient temperature T_{amb} of 45 deg. C and the heat source temperature T_j of 85 deg. C, respectively. Likewise the left and right boundary conditions are the reference temperatures T_{left} and T_{right} of 20 deg. C each.

As expressed by Eq. (2-10) in Chapter 2, the left and right boundary conditions for each material *u* are expressed in the column vectors as

$$\mathbf{f}_{u,j}^{(0)} = (-k_u u_{i,0} + \Delta x^2 \rho_{i,1}^u \quad \Delta x^2 \rho_{i,2}^u \quad \dots \quad \Delta x^2 \rho_{i,m-1}^u \quad -k_u u_{i,m+1} + \Delta x^2 \rho_{i,m}^u)^T \quad (3-2)$$

where k_u is the variable associated with the material *u*. Note that if heat is not generated from material *u*, the constant $\rho_{i,j}^u$ in Eq. (3-2) becomes zero ($j = 1, 2, \dots, m$).

The top and bottom boundary conditions for the combined four layers of materials are given as

$$\mathbf{v}^{(0)} = (v_{0,1} \quad v_{0,2} \quad \dots \quad v_{0,m-1} \quad v_{0,m})^T \quad (3-3)$$

$$\mathbf{w}^{(0)} = (w_{0,1} \quad w_{0,2} \quad \dots \quad w_{0,m-1} \quad w_{0,m})^T \quad (3-4)$$

Note that the superscripts (0) for the above vectors indicate that their element values are given at the start of the S-PSM process.

We apply S-PSM to solve a set of four Poisson thermal conduction equations. We generate finite difference equations that define a connection at the boundary between each pair of adjacent materials. Since each material has its own thermal conductivity, we need to define the equivalent thermal conductivity of the boundary between each pair of adjacent materials.

We consider a pair of material *q* and *r* as a representative case. We set the equivalent thermal conductivity of the boundary

between adjacent materials, q and r of thermal conductivities

k_q and k_r as

$$k_{q,r} = \frac{2k_q k_r}{k_q + k_r} \tag{3-5}$$

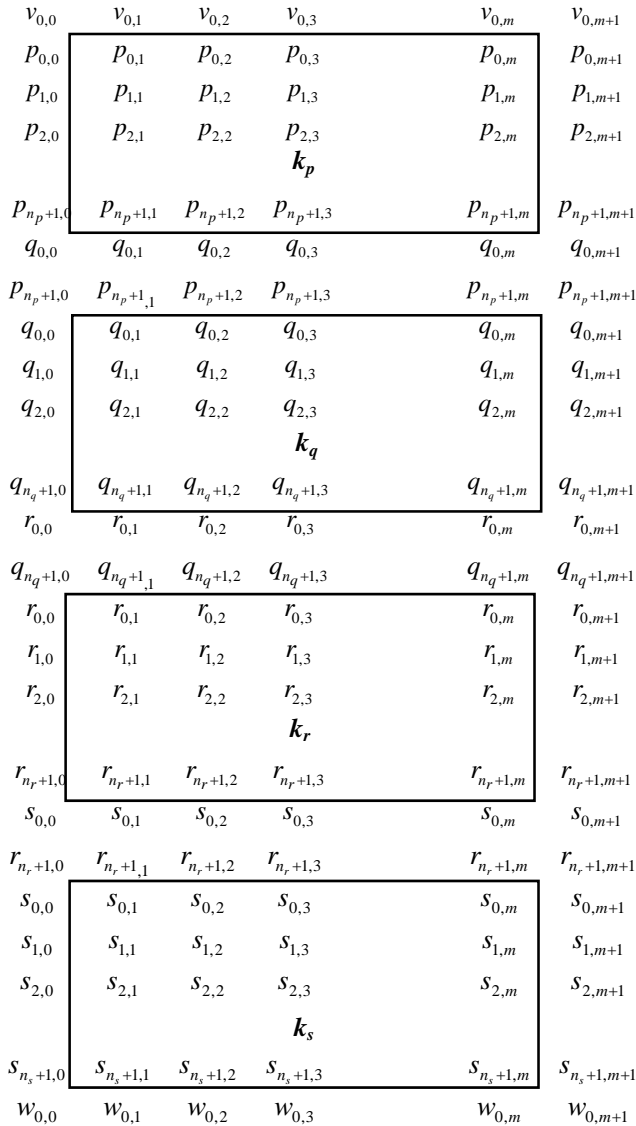


Fig. 3.3. The arrangement of interior grid and boundary points for the four material domains.

At the boundary between each pair of materials, we use the first order approximation for heat conduction as follows.

From the viewpoint of material q , the following difference equation holds at its boundary with material p :

$$k_{p,q}(P_{n_p+1,j} - q_{0,j}) + k_q(q_{0,j-1} - q_{0,j}) + k_q(q_{0,j+1} - q_{0,j}) + k_q(q_{1,j} - q_{0,j}) = \Delta x^2 \rho_{0,j}^q \tag{3-6}$$

Similarly, at its boundary with material r , we have

$$k_q(q_{n_q,j} - q_{n_q+1,j}) + k_q(q_{n_q+1,j-1} - q_{n_q+1,j}) + k_q(q_{n_q+1,j+1} - q_{n_q+1,j}) + k_{q,r}(r_{0,j} - q_{n_q+1,j}) = \Delta x^2 \rho_{n_q+1,j}^q \tag{3-7}$$

Other cases are similarly considered.

Thus, using the variable vector notation

$$\mathbf{u}_i^{(0)} = (u_{i,1} \ u_{i,2} \ u_{i,3} \ \dots \ u_{i,m-1} \ u_{i,m})^T \tag{3-8}$$

we have the following four equations for the pair of adjacent materials, q and r .

$$\left. \begin{aligned} k_{p,q} \mathbf{p}_{n_p+1}^{(e_1)} + A_{q1}^{(0)} \mathbf{q}_0^{(e_2)} + k_q \mathbf{q}_1^{(e_2)} &= \mathbf{f}_{q,0}^{(0)} \\ k_q \mathbf{q}_{n_q}^{(e_2)} + A_{q2}^{(0)} \mathbf{q}_{n_q+1}^{(e_2)} + k_{q,r} \mathbf{r}_0^{(e_3)} &= \mathbf{f}_{q,n_q+1}^{(0)} \\ k_{q,r} \mathbf{r}_{n_q+1}^{(e_2)} + A_{r1}^{(0)} \mathbf{r}_0^{(e_3)} + k_r \mathbf{r}_1^{(e_3)} &= \mathbf{f}_{r,0}^{(0)} \\ k_r \mathbf{r}_{n_r}^{(e_3)} + A_{r2}^{(0)} \mathbf{r}_{n_r+1}^{(e_3)} + k_{r,s} \mathbf{s}_0^{(e_4)} &= \mathbf{f}_{r,n_r+1}^{(0)} \end{aligned} \right\} \tag{3-9}$$

Where

$$\left. \begin{aligned} \mathbf{p}_{n_p+1}^{(e_1)} &= \mathbf{p}_5^{(e_1)}, \quad \mathbf{q}_{n_q}^{(e_2)} = \mathbf{q}_4^{(e_2)}, \quad \mathbf{q}_{n_q+1}^{(e_2)} = \mathbf{q}_5^{(e_2)} \\ \mathbf{r}_{n_r}^{(e_3)} &= \mathbf{r}_4^{(e_3)}, \quad \mathbf{r}_{n_r+1}^{(e_3)} = \mathbf{r}_5^{(e_3)} \end{aligned} \right\} \tag{3-10}$$

$$A_{q1}^{(0)} = \begin{pmatrix} -(k_{p,q} + 3k_q) & k_q & & & \\ k_q & -(k_{p,q} + 3k_q) & k_q & & \\ & k_q & -(k_{p,q} + 3k_q) & k_q & \\ & & \bullet & \bullet & \bullet \\ & & & k_q & -(k_{p,q} + 3k_q) \end{pmatrix} \tag{3-11}$$

$$A_{q2}^{(0)} = \begin{pmatrix} -(3k_q + k_{q,r}) & k_q & & & \\ k_q & -(3k_q + k_{q,r}) & k_q & & \\ & k_q & -(3k_q + k_{q,r}) & k_q & \\ & & \bullet & \bullet & \bullet \\ & & & k_q & -(3k_q + k_{q,r}) \end{pmatrix} \tag{3-12}$$

$$A_{r1}^{(0)} = \begin{pmatrix} -(k_{q,r} + 3k_r) & k_r & & & \\ k_r & -(k_{q,r} + 3k_r) & k_r & & \\ & k_r & -(k_{q,r} + 3k_r) & k_r & \\ & & \bullet & \bullet & \bullet \\ & & & k_r & -(k_{q,r} + 3k_r) \end{pmatrix} \tag{3-13}$$

$$A_{r2}^{(0)} = \begin{pmatrix} -(3k_r + k_{r,s}) & k_r & & & \\ k_r & -(3k_r + k_{r,s}) & k_r & & \\ & k_r & -(3k_r + k_{r,s}) & k_r & \\ & & \bullet & \bullet & \bullet \\ & & & k_r & -(3k_r + k_{r,s}) \end{pmatrix} \tag{3-14}$$

As depicted in Fig. 3.2, many levels of decomposition and merging operations take place but most of those operations occur within each material (for detailed discussions in Chapter 2). So as seen in the above equations and those to follow, the superscripts attached to vectors are at the last levels such as (e) and $(e+1)$. Note that the superscript (0) indicates that the values

given at the beginning of the S-PSM process do not change at the end of the process. Note also that the Eq. (3-10) describes the correspondence between the variable names of each of the two materials (for the reasoning to derive such equations, see Eq. (2-36) of Chapter 2).

On the other hand, we now get the following equations for the second and third material (for the reasoning to derive such equations, see Eq. (2-39) of Chapter 2).

$$\left. \begin{aligned} \mathbf{q}_1^{(e_2)} &= \mathbf{f}_{q,1}^{(e_2+1)} - A_1^{(e_2+1)} \mathbf{q}_0^{(e_2)} - A_2^{(e_2+1)} \mathbf{q}_5^{(e_2)} \\ \mathbf{q}_4^{(e_2)} &= \mathbf{f}_{q,2}^{(e_2+1)} - A_2^{(e_2+1)} \mathbf{q}_0^{(e_2)} - A_1^{(e_2+1)} \mathbf{q}_5^{(e_2)} \end{aligned} \right\} \quad (3-15)$$

$$\left. \begin{aligned} \mathbf{r}_1^{(e_3)} &= \mathbf{f}_{r,1}^{(e_3+1)} - A_1^{(e_3+1)} \mathbf{r}_0^{(e_3)} - A_2^{(e_3+1)} \mathbf{r}_5^{(e_3)} \\ \mathbf{r}_4^{(e_3)} &= \mathbf{f}_{r,2}^{(e_3+1)} - A_2^{(e_3+1)} \mathbf{r}_0^{(e_3)} - A_1^{(e_3+1)} \mathbf{r}_5^{(e_3)} \end{aligned} \right\} \quad (3-16)$$

We repeatedly apply the above procedure for derivation of Eqs. (3-9), (3-10), (3-15), and (3-16) to the remaining material boundaries. We then obtain the following matrix-vector form of the Eq. (3-17) for the three boundaries:

$$\begin{pmatrix} A_{p1}^{(0)} & k_p I & O & O \\ A_{p1}^{(e_1+1)} & I & O & A_2^{(e_1+1)} \\ A_{p1}^{(e_1+1)} & O & I & A_1^{(e_1+1)} \\ O & O & k_p I & A_{p2}^{(0)} \\ & k_{p,q} I & A_{p1}^{(0)} & k_p I \\ & & A_{p1}^{(e_1+1)} & I \\ & & A_{p1}^{(e_1+1)} & O \\ & & O & O \\ & & & k_{p,q} I \\ & & & A_{p1}^{(0)} \\ & & & A_{p1}^{(e_1+1)} \\ & & & A_{p1}^{(e_1+1)} \\ & & & O \\ & & & k_{p,q} I \\ & & & A_{p1}^{(0)} \\ & & & A_{p1}^{(e_1+1)} \\ & & & A_{p1}^{(e_1+1)} \\ & & & O \\ & & & k_{p,q} I \\ & & & A_{p1}^{(0)} \\ & & & A_{p1}^{(e_1+1)} \\ & & & A_{p1}^{(e_1+1)} \\ & & & O \end{pmatrix} \begin{pmatrix} \mathbf{p}_0^{(e_1)} \\ \mathbf{p}_1^{(e_1)} \\ \mathbf{p}_4^{(e_1)} \\ \mathbf{p}_5^{(e_1)} \\ \mathbf{q}_5^{(e_2)} \\ \mathbf{q}_4^{(e_2)} \\ \mathbf{q}_1^{(e_2)} \\ \mathbf{q}_0^{(e_2)} \\ \mathbf{r}_0^{(e_3)} \\ \mathbf{r}_1^{(e_3)} \\ \mathbf{r}_4^{(e_3)} \\ \mathbf{r}_5^{(e_3)} \\ \mathbf{s}_5^{(e_4)} \\ \mathbf{s}_4^{(e_4)} \\ \mathbf{s}_1^{(e_4)} \\ \mathbf{s}_0^{(e_4)} \end{pmatrix} = \begin{pmatrix} k_p \mathbf{v}_0^{(0)} \\ \mathbf{0} \\ \mathbf{0} \\ k_{p,q} \mathbf{q}_0^{(e_2)} \\ k_{q,r} \mathbf{r}_0^{(e_3)} \\ \mathbf{0} \\ \mathbf{0} \\ k_{p,q} \mathbf{p}_5^{(e_1)} \\ k_{q,r} \mathbf{q}_5^{(e_2)} \\ \mathbf{0} \\ \mathbf{0} \\ k_{r,s} \mathbf{s}_0^{(e_4)} \\ \mathbf{0} \\ \mathbf{0} \\ \mathbf{0} \\ k_s \mathbf{w}_0^{(0)} \end{pmatrix} + \begin{pmatrix} \mathbf{f}_{p,0}^{(0)} \\ \mathbf{f}_{p,1}^{(e_1+1)} \\ \mathbf{f}_{p,2}^{(e_1+1)} \\ \mathbf{f}_{p,p+1}^{(0)} \\ \mathbf{f}_{q,0}^{(0)} \\ \mathbf{f}_{q,2}^{(e_2+1)} \\ \mathbf{f}_{q,1}^{(e_2+1)} \\ \mathbf{f}_{q,0}^{(0)} \\ \mathbf{f}_{r,0}^{(0)} \\ \mathbf{f}_{r,1}^{(e_3+1)} \\ \mathbf{f}_{r,2}^{(e_3+1)} \\ \mathbf{f}_{r,n_r+1}^{(0)} \\ \mathbf{f}_{s,0}^{(0)} \\ \mathbf{f}_{s,2}^{(e_4+1)} \\ \mathbf{f}_{s,1}^{(e_4+1)} \\ \mathbf{f}_{s,0}^{(0)} \end{pmatrix} \quad (3-17)$$

3.2.3 System Decomposition and Partial Solutions for Each Subsystem/Material

We decompose Eq. (3-17) into four subsystems of equations that correspond to the four materials.

$$\begin{pmatrix} A_{p1}^{(0)} & k_p I & O & O \\ A_{p1}^{(e_1+1)} & I & O & A_2^{(e_1+1)} \\ A_{p1}^{(e_1+1)} & O & I & A_1^{(e_1+1)} \\ O & O & k_p I & A_{p2}^{(0)} \end{pmatrix} \begin{pmatrix} \mathbf{p}_0^{(e_1)} \\ \mathbf{p}_1^{(e_1)} \\ \mathbf{p}_4^{(e_1)} \\ \mathbf{p}_5^{(e_1)} \end{pmatrix} = \begin{pmatrix} k_p \mathbf{v}_0^{(0)} \\ \mathbf{0} \\ \mathbf{0} \\ k_{p,q} \mathbf{q}_0^{(e_2)} \end{pmatrix} + \begin{pmatrix} \mathbf{f}_{p,0}^{(0)} \\ \mathbf{f}_{p,1}^{(e_1+1)} \\ \mathbf{f}_{p,2}^{(e_1+1)} \\ \mathbf{f}_{p,p+1}^{(0)} \end{pmatrix} \quad (3-18)$$

$$\begin{pmatrix} A_{q2}^{(0)} & k_q I & O & O \\ A_{q1}^{(e_2+1)} & I & O & A_2^{(e_2+1)} \\ A_{q1}^{(e_2+1)} & O & I & A_1^{(e_2+1)} \\ O & O & k_q I & A_{q1}^{(0)} \end{pmatrix} \begin{pmatrix} \mathbf{q}_5^{(e_2)} \\ \mathbf{q}_4^{(e_2)} \\ \mathbf{q}_1^{(e_2)} \\ \mathbf{q}_0^{(e_2)} \end{pmatrix} = \begin{pmatrix} k_{q,r} \mathbf{r}_0^{(e_3)} \\ \mathbf{0} \\ \mathbf{0} \\ k_{p,q} \mathbf{p}_5^{(e_1)} \end{pmatrix} + \begin{pmatrix} \mathbf{f}_{q,n_q+1}^{(0)} \\ \mathbf{f}_{q,2}^{(e_2+1)} \\ \mathbf{f}_{q,1}^{(e_2+1)} \\ \mathbf{f}_{q,0}^{(0)} \end{pmatrix} \quad (3-19)$$

$$\begin{pmatrix} A_{r1}^{(0)} & k_r I & O & O \\ A_{r1}^{(e_3+1)} & I & O & A_2^{(e_3+1)} \\ A_{r1}^{(e_3+1)} & O & I & A_1^{(e_3+1)} \\ O & O & k_r I & A_{r2}^{(0)} \end{pmatrix} \begin{pmatrix} \mathbf{r}_0^{(e_3)} \\ \mathbf{r}_1^{(e_3)} \\ \mathbf{r}_4^{(e_3)} \\ \mathbf{r}_5^{(e_3)} \end{pmatrix} = \begin{pmatrix} k_{q,r} \mathbf{q}_5^{(e_2)} \\ \mathbf{0} \\ \mathbf{0} \\ k_{r,s} \mathbf{s}_0^{(e_4)} \end{pmatrix} + \begin{pmatrix} \mathbf{f}_{r,0}^{(0)} \\ \mathbf{f}_{r,1}^{(e_3+1)} \\ \mathbf{f}_{r,2}^{(e_3+1)} \\ \mathbf{f}_{r,n_r+1}^{(0)} \end{pmatrix} \quad (3-20)$$

$$\begin{pmatrix} A_{s2}^{(0)} & k_s I & O & O \\ A_1^{(e_4+1)} & I & O & A_2^{(e_4+1)} \\ A_2^{(e_4+1)} & O & I & A_1^{(e_4+1)} \\ O & O & k_s I & A_{s1}^{(0)} \end{pmatrix} \begin{pmatrix} \mathbf{s}_5^{(e_4)} \\ \mathbf{s}_4^{(e_4)} \\ \mathbf{s}_1^{(e_4)} \\ \mathbf{s}_0^{(e_4)} \end{pmatrix} = \begin{pmatrix} k_s \mathbf{w}_0^{(0)} \\ \mathbf{0} \\ \mathbf{0} \\ k_{r,s} \mathbf{r}_5^{(e_3)} \end{pmatrix} + \begin{pmatrix} \mathbf{f}_{s,n_s+1}^{(0)} \\ \mathbf{f}_{s,2}^{(e_4+1)} \\ \mathbf{f}_{s,1}^{(e_4+1)} \\ \mathbf{f}_{s,0}^{(0)} \end{pmatrix} \quad (3-21)$$

We denote the inverse matrix of each coefficient matrix of the above equations by the matrix of 16 submatrices of the form B^u as shown below. The partial solutions for each subsystem are given as follows (for the correspondence between the blocks of the inverse matrix above and the B matrix below, See Eqs. (A-1) and (A-3) of Appendix A).

$$\begin{pmatrix} \mathbf{p}_0^{(e_1)} \\ \mathbf{p}_1^{(e_1)} \\ \mathbf{p}_4^{(e_1)} \\ \mathbf{p}_5^{(e_1)} \end{pmatrix} = \begin{pmatrix} B_{1,1}^p & B_{1,2}^p & B_{1,3}^p & B_{1,4}^p \\ B_{2,1}^p & B_{2,2}^p & B_{2,3}^p & B_{2,4}^p \\ B_{3,1}^p & B_{3,2}^p & B_{3,3}^p & B_{3,4}^p \\ B_{4,1}^p & B_{4,2}^p & B_{4,3}^p & B_{4,4}^p \end{pmatrix} \begin{pmatrix} k_p \mathbf{v}_0^{(0)} \\ \mathbf{0} \\ \mathbf{0} \\ k_{p,q} \mathbf{q}_0^{(e_2)} \end{pmatrix} + \begin{pmatrix} \mathbf{f}_{p,0}^{(0)} \\ \mathbf{f}_{p,1}^{(e_1+1)} \\ \mathbf{f}_{p,2}^{(e_1+1)} \\ \mathbf{f}_{p,p+1}^{(0)} \end{pmatrix} \quad (3-22)$$

$$\begin{pmatrix} \mathbf{q}_5^{(e_2)} \\ \mathbf{q}_4^{(e_2)} \\ \mathbf{q}_1^{(e_2)} \\ \mathbf{q}_0^{(e_2)} \end{pmatrix} = \begin{pmatrix} B_{1,1}^q & B_{1,2}^q & B_{1,3}^q & B_{1,4}^q \\ B_{2,1}^q & B_{2,2}^q & B_{2,3}^q & B_{2,4}^q \\ B_{3,1}^q & B_{3,2}^q & B_{3,3}^q & B_{3,4}^q \\ B_{4,1}^q & B_{4,2}^q & B_{4,3}^q & B_{4,4}^q \end{pmatrix} \begin{pmatrix} k_{q,r} \mathbf{r}_0^{(e_3)} \\ \mathbf{0} \\ \mathbf{0} \\ k_{p,q} \mathbf{p}_5^{(e_1)} \end{pmatrix} + \begin{pmatrix} \mathbf{f}_{q,n_q+1}^{(0)} \\ \mathbf{f}_{q,2}^{(e_2+1)} \\ \mathbf{f}_{q,1}^{(e_2+1)} \\ \mathbf{f}_{q,0}^{(0)} \end{pmatrix} \quad (3-23)$$

$$\begin{pmatrix} \mathbf{r}_0^{(e_3)} \\ \mathbf{r}_1^{(e_3)} \\ \mathbf{r}_4^{(e_3)} \\ \mathbf{r}_5^{(e_3)} \end{pmatrix} = \begin{pmatrix} B_{1,1}^r & B_{1,2}^r & B_{1,3}^r & B_{1,4}^r \\ B_{2,1}^r & B_{2,2}^r & B_{2,3}^r & B_{2,4}^r \\ B_{3,1}^r & B_{3,2}^r & B_{3,3}^r & B_{3,4}^r \\ B_{4,1}^r & B_{4,2}^r & B_{4,3}^r & B_{4,4}^r \end{pmatrix} \begin{pmatrix} k_{q,r} \mathbf{q}_5^{(e_2)} \\ \mathbf{0} \\ \mathbf{0} \\ k_{r,s} \mathbf{s}_0^{(e_4)} \end{pmatrix} + \begin{pmatrix} \mathbf{f}_{r,0}^{(0)} \\ \mathbf{f}_{r,1}^{(e_3+1)} \\ \mathbf{f}_{r,2}^{(e_3+1)} \\ \mathbf{f}_{r,n_r+1}^{(0)} \end{pmatrix} \quad (3-24)$$

$$\begin{pmatrix} \mathbf{s}_5^{(e_4)} \\ \mathbf{s}_4^{(e_4)} \\ \mathbf{s}_1^{(e_4)} \\ \mathbf{s}_0^{(e_4)} \end{pmatrix} = \begin{pmatrix} B_{1,1}^s & B_{1,2}^s & B_{1,3}^s & B_{1,4}^s \\ B_{2,1}^s & B_{2,2}^s & B_{2,3}^s & B_{2,4}^s \\ B_{3,1}^s & B_{3,2}^s & B_{3,3}^s & B_{3,4}^s \\ B_{4,1}^s & B_{4,2}^s & B_{4,3}^s & B_{4,4}^s \end{pmatrix} \begin{pmatrix} k_s \mathbf{w}_0^{(0)} \\ \mathbf{0} \\ \mathbf{0} \\ k_{r,s} \mathbf{r}_5^{(e_3)} \end{pmatrix} + \begin{pmatrix} \mathbf{f}_{s,n_s+1}^{(0)} \\ \mathbf{f}_{s,2}^{(e_4+1)} \\ \mathbf{f}_{s,1}^{(e_4+1)} \\ \mathbf{f}_{s,0}^{(0)} \end{pmatrix} \quad (3-25)$$

3.2.4 Merging of Partial Solutions for Each Pair of Adjacent Materials

For the pair of adjacent materials p and q , we extract two equations for variables $\mathbf{p}_5^{(e_1)}$ and $\mathbf{q}_0^{(e_2)}$ from Eqs. (3-22) and (3-23), respectively, and merge them to get Eq. (3-26). Similarly, for the r, s pair, we merge the two equations with respect to $\mathbf{r}_5^{(e_3)}$ and $\mathbf{s}_0^{(e_4)}$ from Eqs. (3-24) and (3-25), and derive Eq. (3-27).

$$\begin{pmatrix} I & O & k_{p,q} B_{1,4}^p & O \\ O & I & k_{p,q} B_{4,4}^p & O \\ O & k_{p,q} B_{3,4}^q & I & O \\ O & k_{p,q} B_{4,4}^q & O & I \end{pmatrix} \begin{pmatrix} \mathbf{p}_5^{(e_1)} \\ \mathbf{q}_0^{(e_2)} \end{pmatrix} = \begin{pmatrix} k_p B_{1,1}^p \mathbf{v}_0^{(0)} \\ k_p B_{4,1}^p \mathbf{v}_0^{(0)} \\ k_{q,r} B_{4,1}^q \mathbf{r}_0^{(e_3)} \\ k_{q,r} B_{1,1}^q \mathbf{r}_0^{(e_3)} \end{pmatrix} + \begin{pmatrix} \mathbf{ff}_{p0} \\ \mathbf{ff}_{p5} \\ \mathbf{ff}_{q0} \\ \mathbf{ff}_{q5} \end{pmatrix} \quad (3-26)$$

$$\begin{pmatrix} I & O & k_{r,s} B_{1,4}^r & O \\ O & I & k_{r,s} B_{4,4}^r & O \\ O & k_{r,s} B_{3,4}^s & I & O \\ O & k_{r,s} B_{4,4}^s & O & I \end{pmatrix} \begin{pmatrix} \mathbf{r}_5^{(e_3)} \\ \mathbf{s}_0^{(e_4)} \end{pmatrix} = \begin{pmatrix} k_{q,r} B_{1,1}^r \mathbf{q}_5^{(e_2)} \\ k_{q,r} B_{4,1}^r \mathbf{q}_5^{(e_2)} \\ k_s B_{4,1}^s \mathbf{w}_0^{(0)} \\ k_s B_{1,1}^s \mathbf{w}_0^{(0)} \end{pmatrix} + \begin{pmatrix} \mathbf{ff}_{r0} \\ \mathbf{ff}_{r5} \\ \mathbf{ff}_{s0} \\ \mathbf{ff}_{s5} \end{pmatrix} \quad (3-27)$$

where

$$\left. \begin{aligned} \mathbf{ff}_{p0} &= B_{1,1}^p \mathbf{f}_{p,0}^{(0)} + B_{1,2}^p \mathbf{f}_{p,1}^{(e_1+1)} + B_{1,3}^p \mathbf{f}_{p,2}^{(e_1+1)} + B_{1,4}^p \mathbf{f}_{p,n_p+1}^{(0)} \\ \mathbf{ff}_{p5} &= B_{4,1}^p \mathbf{f}_{p,0}^{(0)} + B_{4,2}^p \mathbf{f}_{p,1}^{(e_1+1)} + B_{4,3}^p \mathbf{f}_{p,2}^{(e_1+1)} + B_{4,4}^p \mathbf{f}_{p,n_p+1}^{(0)} \\ \mathbf{ff}_{q0} &= B_{4,1}^q \mathbf{f}_{q,n_q+1}^{(0)} + B_{4,2}^q \mathbf{f}_{q,2}^{(e_2+1)} + B_{4,3}^q \mathbf{f}_{q,1}^{(e_2+1)} + B_{4,4}^q \mathbf{f}_{q,0}^{(0)} \\ \mathbf{ff}_{q5} &= B_{1,1}^q \mathbf{f}_{q,n_q+1}^{(0)} + B_{1,2}^q \mathbf{f}_{q,2}^{(e_2+1)} + B_{1,3}^q \mathbf{f}_{q,1}^{(e_2+1)} + B_{1,4}^q \mathbf{f}_{q,0}^{(0)} \\ \mathbf{ff}_{r0} &= B_{1,1}^r \mathbf{f}_{r,0}^{(0)} + B_{1,2}^r \mathbf{f}_{r,1}^{(e_3+1)} + B_{1,3}^r \mathbf{f}_{r,2}^{(e_3+1)} + B_{1,4}^r \mathbf{f}_{r,n_r+1}^{(0)} \\ \mathbf{ff}_{r5} &= B_{4,1}^r \mathbf{f}_{r,0}^{(0)} + B_{4,2}^r \mathbf{f}_{r,1}^{(e_3+1)} + B_{4,3}^r \mathbf{f}_{r,2}^{(e_3+1)} + B_{4,4}^r \mathbf{f}_{r,n_r+1}^{(0)} \\ \mathbf{ff}_{s0} &= B_{4,1}^s \mathbf{f}_{s,n_s+1}^{(0)} + B_{4,2}^s \mathbf{f}_{s,2}^{(e_4+1)} + B_{4,3}^s \mathbf{f}_{s,1}^{(e_4+1)} + B_{4,4}^s \mathbf{f}_{s,0}^{(0)} \\ \mathbf{ff}_{s5} &= B_{1,1}^s \mathbf{f}_{s,n_s+1}^{(0)} + B_{1,2}^s \mathbf{f}_{s,2}^{(e_4+1)} + B_{1,3}^s \mathbf{f}_{s,1}^{(e_4+1)} + B_{1,4}^s \mathbf{f}_{s,0}^{(0)} \end{aligned} \right\} \quad (3-28)$$

As both of the above coefficient matrices are of special structure, their inverse matrices are expressed as shown below with two full middle columns of submatrices of the forms B^{pq} and B^{rs} , respectively. The partial solutions for each pair of materials are now obtained as follows (See Eq. (A-4) of Appendix A).

$$\begin{pmatrix} \mathbf{p}_0^{(e_1)} \\ \mathbf{p}_5^{(e_1)} \\ \mathbf{q}_0^{(e_2)} \\ \mathbf{q}_5^{(e_2)} \end{pmatrix} = \begin{pmatrix} I & B_{1,1}^{pq} & B_{2,1}^{pq} & O \\ O & B_{1,2}^{pq} & B_{2,2}^{pq} & O \\ O & B_{1,3}^{pq} & B_{2,3}^{pq} & O \\ O & B_{1,4}^{pq} & B_{2,4}^{pq} & I \end{pmatrix} \begin{pmatrix} k_p B_{1,1}^p \mathbf{v}_0^{(0)} \\ k_p B_{4,1}^p \mathbf{v}_0^{(0)} \\ k_{q,r} B_{4,1}^q \mathbf{r}_0^{(e_3)} \\ k_{q,r} B_{1,1}^q \mathbf{r}_0^{(e_3)} \end{pmatrix} + \begin{pmatrix} \mathbf{ff}_{p0} \\ \mathbf{ff}_{p5} \\ \mathbf{ff}_{q0} \\ \mathbf{ff}_{q5} \end{pmatrix} \quad (3-29)$$

$$\begin{pmatrix} \mathbf{r}_0^{(e_3)} \\ \mathbf{r}_5^{(e_3)} \\ \mathbf{s}_0^{(e_4)} \\ \mathbf{s}_5^{(e_4)} \end{pmatrix} = \begin{pmatrix} I & B_{1,1}^{rs} & B_{2,1}^{rs} & O \\ O & B_{1,2}^{rs} & B_{2,2}^{rs} & O \\ O & B_{1,3}^{rs} & B_{2,3}^{rs} & O \\ O & B_{1,4}^{rs} & B_{2,4}^{rs} & I \end{pmatrix} \begin{pmatrix} k_{q,r} B_{1,1}^r \mathbf{q}_5^{(e_2)} \\ k_{q,r} B_{4,1}^r \mathbf{q}_5^{(e_2)} \\ k_s B_{4,1}^s \mathbf{w}_0^{(0)} \\ k_s B_{1,1}^s \mathbf{w}_0^{(0)} \end{pmatrix} + \begin{pmatrix} \mathbf{ff}_{r0} \\ \mathbf{ff}_{r5} \\ \mathbf{ff}_{s0} \\ \mathbf{ff}_{s5} \end{pmatrix} \quad (3-30)$$

3.2.5 Final Solutions

Finally, for the two pairs of materials p and q , and of r and s , we extract equations with respect to variables $\mathbf{q}_5^{(e_2)}$ and $\mathbf{r}_0^{(e_3)}$ from Eqs. (3-29) and (3-30). Their merging then produces the following equation.

$$\begin{pmatrix} I & k_{q,r} (B_{2,4}^{pq} B_{4,1}^q + B_{1,1}^q) \\ k_{q,r} (B_{1,1}^{rs} B_{4,1}^r + B_{1,1}^r) & I \end{pmatrix} \begin{pmatrix} \mathbf{q}_5^{(e_2)} \\ \mathbf{r}_0^{(e_3)} \end{pmatrix} = - \begin{pmatrix} k_p B_{1,4}^p B_{4,1}^p \mathbf{v}_0^{(0)} \\ k_s B_{2,1}^s B_{4,1}^s \mathbf{w}_0^{(0)} \end{pmatrix} + \begin{pmatrix} \mathbf{ff}_{pq} \\ \mathbf{ff}_{rs} \end{pmatrix} \quad (3-31)$$

where

$$\left. \begin{aligned} \mathbf{ff}_{pq} &= B_{1,4}^{pq} \mathbf{ff}_{p5} + B_{2,4}^{pq} \mathbf{ff}_{q0} + \mathbf{ff}_{q5} \\ \mathbf{ff}_{rs} &= \mathbf{ff}_{r0} + B_{1,1}^{rs} \mathbf{ff}_{r5} + B_{2,1}^{rs} \mathbf{ff}_{s0} \end{aligned} \right\} \quad (3-32)$$

We then take the inverse matrix of the coefficient matrix of Eq. (3-31) and derive the final solutions for variables $\mathbf{q}_5^{(e_2)}$ and $\mathbf{r}_0^{(e_3)}$ as follows (See Eq. (A-6) of Appendix A).

$$\left. \begin{aligned} \mathbf{q}_5^{(e_2)} &= -D_1 (B_{1,4}^{pq} (B_{4,1}^p \mathbf{v}_0^{(0)})) - D_2 (B_{2,1}^{rs} (B_{4,1}^s \mathbf{w}_0^{(0)})) + D_1 \mathbf{ff}_{pq} + D_2 \mathbf{ff}_{rs} \\ \mathbf{r}_0^{(e_3)} &= -D_3 (B_{1,4}^{pq} (B_{4,1}^p \mathbf{v}_0^{(0)})) - D_4 (B_{2,1}^{rs} (B_{4,1}^s \mathbf{w}_0^{(0)})) + D_3 \mathbf{ff}_{pq} + D_4 \mathbf{ff}_{rs} \end{aligned} \right\} \quad (3-33)$$

where

$$\left. \begin{aligned} D_1 &= [I - k_{q,r} k_{q,r} (B_{2,4}^{pq} B_{4,1}^q + B_{1,1}^q) (B_{1,1}^{rs} B_{4,1}^r + B_{1,1}^r)]^{-1} \\ D_2 &= -k_{q,r} D_1 (B_{2,4}^{pq} B_{4,1}^q + B_{1,1}^q) \\ D_4 &= [I - k_{q,r} k_{q,r} (B_{1,1}^{rs} B_{4,1}^r + B_{1,1}^r) (B_{2,4}^{pq} B_{4,1}^q + B_{1,1}^q)]^{-1} \\ D_3 &= -k_{q,r} D_4 (B_{1,1}^{rs} B_{4,1}^r + B_{1,1}^r) \end{aligned} \right\} \quad (3-34)$$

3.2.6 Back Substitution

The above solutions are now substituted into Eqs. (3-29) and (3-30) to find solutions for

$\mathbf{p}_0^{(e_1)}$, $\mathbf{p}_5^{(e_1)}$, $\mathbf{q}_0^{(e_2)}$, $\mathbf{r}_5^{(e_3)}$, $\mathbf{s}_0^{(e_4)}$ and $\mathbf{s}_5^{(e_4)}$. These solutions are then back substituted into Eqs. (3-22), (3-23), (3-24) and (3-25) and the solutions for the remaining variables are obtained, as depicted Fig. 3.4. It should be noted that we need one more step to find solutions for the variables associated with each material. Along a similar line of equation derivations given above, this can be done by way of repeated substitutions of the values for relevant variables into certain equations (See Eqs. (2-37), (2-40), and (2-41) of Chapter 2 for more detail).

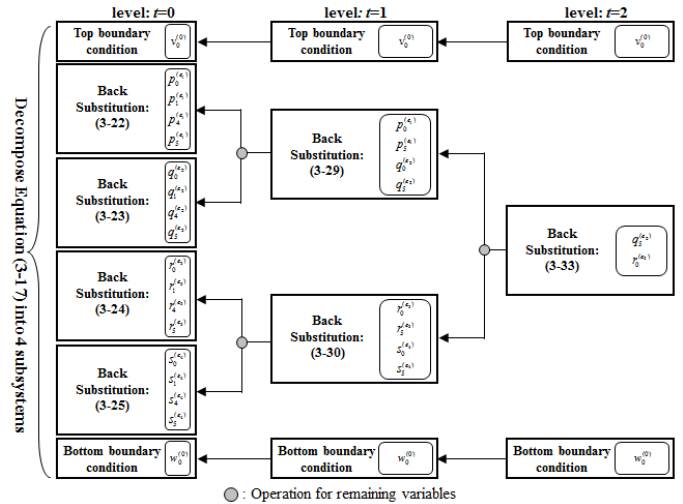


Fig. 3.4: An overall computation flow with relevant equation numbers of a S-PSM-based back substitution process of Poisson thermal conduction thermal equations for four materials.

3.3 Verification

We applied the above mentioned technique to a simplified model of four layer materials of different thermal conductivities, as depicted in Fig. 3.1. The experimental results revealed that our method ran 70 times faster, required 3 times less memory, and an order of magnitude smaller residual than LUD. They also showed that the technique achieved up to 3 times speed-up and used 1.8 times smaller memory than ICCG [11].

IV. EXTENSION TO MULTI-LAYER ANALYSIS

We improved our S-PSM program in order to deal with

multi-layer structures which are composed of a large number of materials. The number of layers (materials) is expressed as a symbol NL ($NL=2^{e+2}$, e is positive integer). The overall computation flow of an S-PSM based solution process is similar to that depicted in Fig. 3.1. It has a binary tree structure. The depth of the tree is equal to $e+2$. In this chapter, we summarize the computation flow as follows.

- (1) **Combining:** The solution of the system of linear equations for each material is obtained corresponding to Eqs. (3-15) and (3-16). Moreover the four equations for each pair of adjacent materials at its boundary are obtained corresponding to Eqs. (3-9) and (3-10). The above procedure is applied repeatedly to all materials and their boundaries. By combining these equations, the matrix-vector form which expresses the whole system is obtained corresponding to Eq. (3-17).
- (2) **Decomposition:** The whole system obtained in the step (1) is decomposed into NL subsystems of equations that correspond to the NL materials. Note that they are equivalent to Eqs. (3-18), (3-19), (3-20) and (3-21). Moreover the partial solution for each subsystem is obtained by the inverse matrix of each coefficient matrix (*See Case 1 and Case 2 of Appendix A*). Note that they are equivalent to Eqs. (3-22), (3-23), (3-24) and (3-25).
- (3) **Low-level merging:** The each pair of partial solutions which obtained in the step (2) is merged into an upper level subsystem. This procedure is applied repeatedly, and $NL/2$ upper level subsystems are obtained. Note that they are equivalent to Eqs. (3-26) and (3-27). Moreover the partial solution for each upper level subsystem is obtained by the inverse matrix of each coefficient matrix (*See Case 3 of Appendix A*). Note that they are equivalent to Eqs. (3-29), and (3-30).
- (4) **Mid-level merging:** The each pair of partial solutions which obtained in the step (3) is merged into a more upper level subsystem. This procedure is applied repeatedly, and $NL/4$ more upper level subsystems are obtained. Note that they are equivalent to Eqs. (3-26) and (3-27). Moreover the partial solution for each more upper level subsystem is obtained by the inverse matrix of each coefficient matrix (*See Case 3 of Appendix A*). Note that they are equivalent to Eqs. (3-29), and (3-30). The two partial solutions are obtained by applying these operations repeatedly with a bottom-up approach.
- (5) **Final Solution:** The pair of the partial solutions which obtained finally in the step (4) is merged into an uppermost system. Note that it corresponds to Eq. (3-31). Moreover the solution for the uppermost system is obtained by the inverse matrix of the coefficient matrix (*See Case 4 of Appendix A*). Note that it corresponds to Eq. (3-33).
- (6) **Back substitution:** The solutions for the remaining variables are derived by repeating back substitution as described in section 3.2.6.

We applied our S-PSM program which is extended as above to multi-layer thermal analysis for VLSI chips and evaluated the performance of our technique.

As an example of multi-layer thermal analysis, we deal with internal temperature rise due to Joule heating described by Im, et al. [7]. Figure 5.1, Figure 5.2, and Figure 5.3 depict the simulation models which correspond to 8-layer structure, 16-layer structure and 32-layer structure, respectively. In the example of 32-layer structure, its simulation model consists of equivalent package layer, equivalent passivation layer, five global interconnect layers, nine intermediate interconnect layers and local interconnect layer (M1) over the unit-cell. Moreover an interlayer dielectric (ILD) layer is placed between each pair of adjacent interconnect layer. The values of simulation parameters (interconnect thickness, ILD thickness, ILD thermal conductivity (k_{ILD}), etc.) and thermal parameters (resistivity, maximum current density, etc.) are taken from Im, *et al.* [7]. Also the boundary conditions are set in the same as way. Furthermore, since each ILD layer, package layer, and passivation layer do not have Joule heating effect, they are described by Poisson equations of which the right hand side is equal to zero. Since each interconnect layer has Joule heating effect, it is described by Poisson equation. Thus whole phenomenon of thermal conduction and heat generation are described by a set of Poisson equations.

With the parameter settings mentioned above, we applied we perform two-dimensional steady-state thermal analysis and checked the temperature rise with respect to the junction temperature ($\Delta T_{max} = T_{max} - T_j$). Figure 5.4 depicts the temperature rises for the 32-layer structure obtained by our program. It shows different temperature rise depending on copper technology used. The copper technologies used are 22/32/45/65nm processes. Moreover, we calculated the values of temperature rises for the example of thermal analysis which is taken from Im, et al. [7] by using our program, and compared the results to those of [7]. Both resemble very close to each other, as depicted in Fig. 5.5. This implies that our technique produces correct results.

We perform multi-layer thermal analysis using the simulation models for 8-layer, 16-layer and 32-layer structures in order to evaluate the performance of our technique. We use simulation parameters and thermal parameters of 22nm copper technology [7]. In the same way as the chip level thermal analysis mentioned in the previous subsection, the number of Y-direction grids (h) and the number of X-direction grids (g) are set so that the mesh size of Y-direction is equal to that of X-direction ($\Delta x = \Delta y$).

Table 5.1 shows the CPU times required and the residuals produced by our program, ICCG method and CG method in the simulation model of 8-layer structure. Note that conventional CG (Conjugate Gradient) method is borrowed from LAPACK packages [5] in the same way as ICCG method. The ICCG method is more than five times faster than the CG method because of its pre-conditioner. The results demonstrate that for the largest grid ($h=256$, $g=1680$, matrix size= $h \times g=430080$), our program ran 2.93 and 5.4 times faster while keeping smaller residuals by 6 and 2 order of magnitudes, respectively, than

V. EXPERIMENTS RESULTS

ICCG. The memory usage of our program is 1.31 times less than that by ICCG.

Table 5.2 shows the CPU times required and the residuals produced by our program, ICCG method and CG method in the simulation model of 16-layer structure. The results demonstrate that for the largest grid ($h=256, g=2464$, matrix size= $h \times g=630784$), our program ran 3.0 and 5.7 times faster while keeping smaller residuals by 5 and 1 order of magnitudes, respectively, than ICCG. The memory usage of our program is 1.02 times less than that by ICCG.

Table 5.3 shows the CPU times required and the residuals produced by our program, ICCG method and CG method in the simulation model of 32-layer structure. The results demonstrate that for the largest grid ($h=256, g=3776$, matrix size= $h \times g=966656$), our program ran 3.25 and 6.4 times faster while keeping smaller residuals by 5 and 1 order of magnitudes, respectively, than ICCG.

The summary of the results mentioned above is as follows: (1) With the increase of layers of simulation model becomes larger, the solution speed by our technique becomes faster than that of ICCG. (2) The residuals are more than an order of magnitudes smaller than that of ICCG.

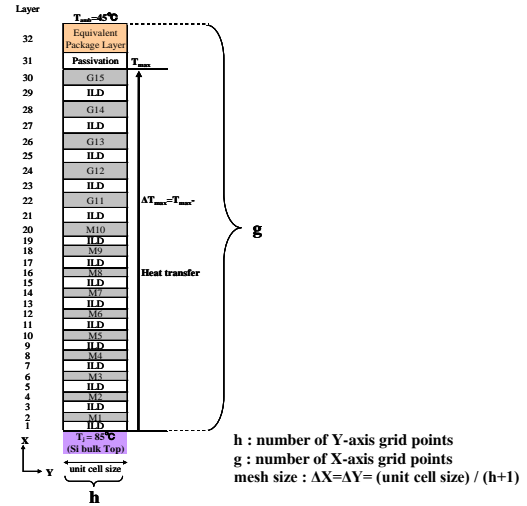


Fig. 5.3: Thermal simulation model for 32-layer structure.

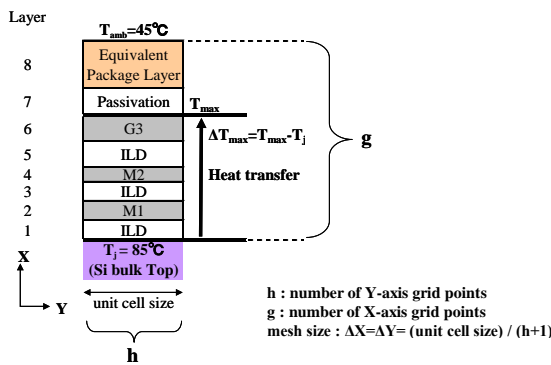


Fig. 5.1: Thermal simulation model for 8-layer structure.

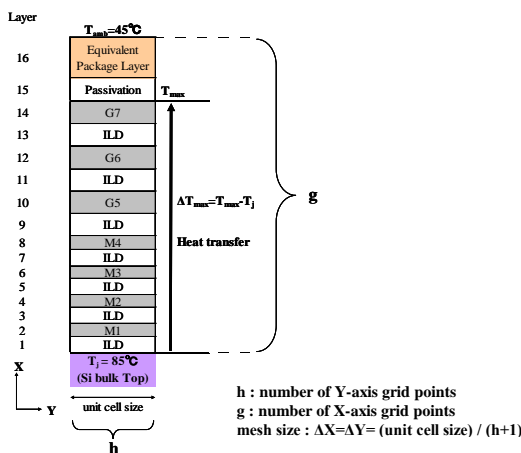


Fig. 5.2: Thermal simulation model for 16-layer structure.

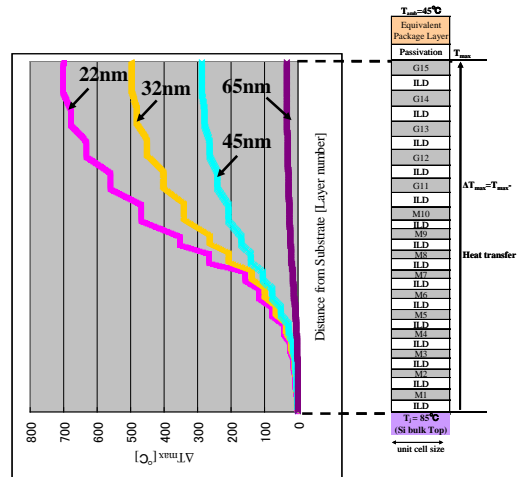


Fig. 5.4: Temperature rises for the 32-layer structure obtained by our program. The copper technologies used are 22/32/45/65nm processes.

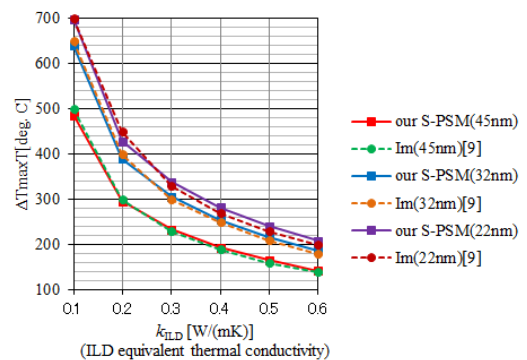


Fig. 5.5: Comparison between temperature rises obtained by our program, and those of [7].

VI. CONCLUSIONS

We have presented a new technique of thermal analysis for multi-layer VLSI chips. After modeling multiple layers of materials of different heat conductivities by a set of Poisson equations, it discretizes the equations and applies S-PSM to the resulting systems of linear equations.

We have applied our technique to two-dimensional, steady-state heat conduction analysis for Joule heating problem of multi-layer interconnect structure, and compared our program to ICCG method. The experimental results demonstrate the superiority of our program by the factors of 3.25 and 6.4 while keeping smaller residuals by 5 and 1 order(s) of magnitude, respectively. They reveal the superiority of our technique in the thermal analysis for multi-layer VLSI chips.

Research on the extension of our technique to three dimensional analysis and transient heat conduction analysis for multi-layer materials of more complex shapes is under way.

APPENDICES

A. Appendix A: Formula for inverse matrices

Case 1: The inverse matrix of the coefficient matrix for each of Eqs. (3-18), (3-19), (3-20) and (3-21).

$$\begin{pmatrix} A_1 & I & O & O \\ A_2 & I & O & A_3 \\ A_3 & O & I & A_2 \\ O & O & K & A_4 \end{pmatrix}^{-1} = \begin{pmatrix} B_{1,1} & B_{1,2} & B_{1,3} & B_{1,4} \\ B_{2,1} & B_{2,2} & B_{2,3} & B_{2,4} \\ B_{3,1} & B_{3,2} & B_{3,3} & B_{3,4} \\ B_{4,1} & B_{4,2} & B_{4,3} & B_{4,4} \end{pmatrix} \quad (\text{A-1})$$

where

$$\left. \begin{aligned} C &= (I - A_2 A_1^{-1})^{-1} \\ B_{4,4} &= (A_4 - K(A_2 + A_3 A_1^{-1} C A_3))^{-1} \\ B_{3,3} &= A_4 B_{4,4}, \quad B_{3,4} = (I - A_4 B_{4,4}) K^{-1} \\ B_{4,3} &= -K B_{4,4}, \quad B_{1,4} = A_1^{-1} C A_3 B_{4,4} \\ B_{1,3} &= -K B_{1,4}, \quad B_{2,4} = -(I + A_2 A_1^{-1} C) A_3 B_{4,4} \\ B_{2,3} &= -K B_{2,4}, \quad B_{3,1} = -B_{3,3} A_3 A_1^{-1} C \\ B_{3,2} &= -B_{3,1}, \quad B_{4,1} = -B_{4,3} A_3 A_1^{-1} C \\ B_{4,2} &= -B_{4,1}, \quad B_{1,1} = (I + K B_{1,4} A_3) A_1^{-1} C \\ B_{1,2} &= -B_{1,1}, \quad B_{2,1} = -C A_2 A_1^{-1} - B_{2,3} A_3 A_1^{-1} C \\ B_{2,2} &= I - K B_{2,1} \end{aligned} \right\} \quad (\text{A-2})$$

Case 2: The inverse matrix of the coefficient matrix for each of Eqs. (3-18), (3-19), (3-20) and (3-21).

$$\begin{pmatrix} A_1 & K_1 & O & O \\ A_2 & I & O & A_3 \\ A_3 & O & I & A_2 \\ O & O & K_2 & A_4 \end{pmatrix}^{-1} = \left(\begin{pmatrix} K_1 & O & O & O \\ O & I & O & O \\ O & O & I & O \\ O & O & O & I \end{pmatrix} \begin{pmatrix} K_1^{-1} A_1 & I & O & O \\ A_2 & I & O & A_3 \\ A_3 & O & I & A_2 \\ O & O & K_2 & A_4 \end{pmatrix} \right)^{-1} \\ = \begin{pmatrix} K_1^{-1} A_1 & I & O & O \\ A_2 & I & O & A_3 \\ A_3 & O & I & A_2 \\ O & O & K_2 & A_4 \end{pmatrix}^{-1} \begin{pmatrix} K_1^{-1} & O & O & O \\ O & I & O & O \\ O & O & I & O \\ O & O & O & I \end{pmatrix} \quad (\text{A-3})$$

Case 3: The inverse matrix of the coefficient matrix for each of Eqs. (3-26) and (3-27).

$$\begin{pmatrix} I & O & A_3 & O \\ O & I & A_4 & O \\ O & A_1 & I & O \\ O & A_2 & O & I \end{pmatrix}^{-1} = \begin{pmatrix} I & B_1 & B_5 & O \\ O & B_2 & B_6 & O \\ O & B_3 & B_7 & O \\ O & B_4 & B_8 & I \end{pmatrix} \quad (\text{A-4})$$

where

$$\left. \begin{aligned} B_2 &= (I - A_4 A_1)^{-1}, \quad B_3 = -B_7 A \\ B_4 &= -A_2 B_2, \quad B_5 = -A_3 B_7 \\ B_7 &= (I - A_1 A_4)^{-1}, \quad B_1 = -B_5 A_1 \\ B_6 &= -B_2 A_4, \quad B_8 = -B_4 A_4 \end{aligned} \right\} \quad (\text{A-5})$$

Case 4: The inverse matrix of the coefficient matrix for Eq. (3-31)

$$\begin{pmatrix} I & A_1 \\ A_2 & I \end{pmatrix}^{-1} = \begin{pmatrix} B_{1,1} & B_{1,2} \\ B_{2,1} & B_{2,2} \end{pmatrix} \quad (\text{A-6})$$

where

$$\left. \begin{aligned} B_{1,1} &= (I - A_1 A_2)^{-1} \\ B_{1,2} &= -B_{1,1} A_1 \\ B_{2,2} &= (I - A_2 A_1)^{-1} \\ B_{2,1} &= -B_{2,2} A_2 \end{aligned} \right\} \quad (\text{A-7})$$

ACKNOWLEDGMENT

The authors would like to express their gratitude to the deceased Prof. Kazuo Nakajima (University of Maryland College Park) for years of collaboration and advice.

REFERENCES

- [1] Y. K. Cheng, P. Raha, C. C. Teng, E. Rosebaum, and S. M. Kang, "ILLIADS-T: An Electrothermal Timing Simulator for Temperature-sensitive Reliability Diagnosis of CMOS VLSI Chips," *IEEE Trans. on Computer-Aided Design of Integrated Circuits and Systems*, Vol. 17, No. 8, pp. 661-681, Aug. 1998.
- [2] T. Y. Chiang, K. Banerjee, and K. C. Saraswat, "Compact Modeling and SPICE-Based Simulation for Electrothermal Analysis of Multilevel ULSI Interconnects," *Proc. IEEE Int'l Conf. on Computer-Aided Design*, San Jose, CA, Nov. 2001, pp. 165-172.
- [3] T. Hiramoto, M. Osano, and K. Oshima, "Symbolic PSM Solver for the Finite Difference Equations Derived from the Poisson Equation," *Computational Fluid Dynamics Jour.*, Vol. 12, No. 1, pp. 19-28, Apr. 2003.
- [4] <http://www.ansys.com/solutions/multiple-physics.asp>.
- [5] <http://www.mgnet.org/mgnet/Codes/laspack>.
- [6] W. Huang, M. R. Stan, K. Skadron, K. Sankaranarayanan, S. Ghosh, and S. Velusamy, "Compact Thermal Modeling for Temperature Aware Design," *Proc. 41st Design Automation Conf.*, San Diego, CA, June 2004, pp. 878-883.
- [7] S. Im, N. Srivastava, K. Banerjee, and K. E. Goodson, "Scaling Analysis of Multilevel Interconnect Temperatures for High-performances ICs," *IEEE Trans. on Electron Devices*, Vol. 52, No. 12, pp. 2710-2717, Dec. 2005.
- [8] P. Li, L. T. Pileggi, M. Asheghi, and R. Chandra, "IC Thermal Simulation and Modeling via Efficient Multigrid-based Approaches," *IEEE Trans. on*

Computer-Aided Design of Integrated Circuits and Systems, vol. 25, No. 9, pp.1763-1776, Sept. 2006.

[9] L. Miao, Z. Runde, and G. Yuanqing, "A New Electro-thermal Simulator Based on Relaxation Method for Integrated Circuits with Distributed Temperatures," *Proc. Int'l Conf. on Design Automation*, Beijing, China, Aug. 2000, [Link] <http://www.ifip.or.at/con2000/icda2000/icda-11-3.pdf>.

[10] K. Nakabayashi, T. Nakabayashi, and K. Nakajima, "Very Fast Chip-level Thermal Analysis," *Proc. 13th Int'l Workshop on Thermal Investigate of ICs and Systems*, Budapest, Hungary, Sept. 2007, pp. 82-87.

[11] K. Nakabayashi, K. Nakajima, and H. Iida, "A New Technique of Multi-layer Thermal Analysis for VLSI Chips," *Proc. 9th WSEAS International Conference on Mathematical Methods and Computational Techniques in Electrical Engineering*, Arcachon, France, Oct. 2007, pp. 24-30.

[12] M. Osano, K. Nakajima, and M. Tanimoto, "A New Efficient Solution Method for a System of Linear Equations: Partially Solving Method (PSM)," *Japan Jour. of Industrial Math.*, Vol. 13, No. 2, pp. 243-256, June 1996.

[13] M. Pedram, and S. Nazarin, "Thermal Modeling, Analysis, and Management in VLSI Circuits: Principles and Methods," *Proceedings of the IEEE*, Vol. 94, No. 8, pp. 1487-1501, Aug. 2006.

[14] T-Y. Wang and C. C-P. Chen, "3-D Thermal-ADI: a Linear-Time Chip Level Transient Thermal Simulator," *IEEE Trans. on Computer-Aided Design of Integrated Circuits and Systems*, Vol. 21, No. 12, pp. 1434-1445, Dec. 2002.

[15] B. Wang and P. Mazumder, "Accelerated Chip-Level Thermal Analysis Using Multilayer Green's Function," *IEEE Trans. on Computer-Aided Design of Integrated Circuits and Systems*, Vol. 26, No. 2, pp. 325-344, Feb. 2007.

[16] Y. Yang, Z. P. Gu, C. Zhu, R. P. Dick, and L. Shang, "ISAC: Integrated Space and Time Adaptive Chip-Package Thermal Analysis," *IEEE Transactions Computer-Aided Design of Integrated Circuits and Systems*, Vol. 26, No. 1, pp. 86-99, Jan. 2007

[17] W. Huang, S. Ghosh, S. Velusamy, K. Sankaranarayanan, K. Skadron, and M. R. Stan, "HotSpot: A Compact Thermal Modeling Methodology for Early-Stage VLSI Design," *IEEE Trans. on Very Large Scale Integration (VLSI) Systems*, Vol. 14, No. 5, pp. 501-513, MAY 2006.

[18] L. Codecasa, V. d'Alessandro, A. Magnani, N. Rinaldi, and P. J. Zampardi, "Fast novel thermal analysis simulation tool for integrated circuits (FANTASTIC)," *Proc. 20th Int'l Workshop on Thermal Investigate of ICs and Systems*, London, UK, Sept. 2014, pp. 1-6.



Keiji Nakabayashi received the B.S. degree in mathematics from University of Tsukuba, Tsukuba, Japan, in 1985, and received the Ph.D. degree in information engineering from Nara Institute of Science and Technology, Nara, Japan, in 2010. He is currently a researcher with Integration Technology, Co., Ltd., Wako, Saitama, Japan. He was a visiting researcher with the Department of Electrical and Computer Engineering, University of Maryland College Park, MD, USA in 2006. From 2010 to 2012, he was a researcher with Kobe University, Japan. His current research interests include physical-level modeling and simulation techniques for VLSI design in Automotive Electronics, electro-thermal field solver, electro-mechanical solver, and a broad range of numerical methods.

Dr. Nakabayashi was a recipient of the Best Paper Award at the 2012 American Conference on Applied Mathematics, the Best Student Paper Award at the 9th WSEAS International Conference on Mathematical Methods and Computational Techniques in Electrical Engineering in 2007.

Table 5.1: [8-layer structure]: Processing CPU times / Residuals / Memory of S-PSM, ICCG, and CG for difference arrangements grid points.

Number of grid points			S-PSM			ICCG (EPS=1.0E-6)		ICCG (EPS=1.0E-10)			CG (EPS=1.0E-6)		CG (EPS=1.0E-10)		
matrix size (h*g)	h	g	CPU (sec)	Residual	Memory (MB)	CPU (sec)	Residual	CPU (sec)	Residual	Memory (MB)	CPU (sec)	Residual	CPU (sec)	Residual	Memory (MB)
1920	16	120	0.02 (1.0)	1.80E-16	6.7 (1.0)	0.03 (2.07)	9.6E-07	0.04 (2.9)	4.5E-11	6.0 (0.90)	0.15 (9.7)	9.8E-07	0.25 (16.8)	5.6E-11	5.7 (0.86)
7168	32	224	0.08 (1.0)	2.90E-15	11.2 (1.0)	0.18 (2.35)	8.7E-07	0.27 (3.6)	6.6E-11	7.6 (0.68)	1.2 (16.0)	9.3E-07	2.15 (28.6)	8.8E-11	6.5 (0.58)
27648	64	432	0.69 (1.0)	1.10E-14	31.0 (1.0)	1.64 (2.38)	9.4E-07	2.72 (3.9)	8.3E-11	10.7 (0.35)	13.2 (19.1)	9.8E-07	24.61 (35.7)	9.3E-11	8.0 (0.26)
108544	128	848	4.36 (1.0)	4.90E-14	40.0 (1.0)	10.8 (2.49)	9.5E-07	18.9 (4.3)	9.1E-11	26.1 (0.65)	97.3 (22.3)	9.7E-07	199.7 (45.8)	9.9E-11	15.7 (0.39)
430080	256	1680	24.7 (1.0)	4.80E-13	67.1 (1.0)	72.22 (2.93)	9.4E-07	133.1 (5.4)	9.8E-11	87.9 (1.31)	712.2 (28.9)	9.9E-07	1477.3 (59.9)	9.9E-11	46.7 (0.70)

Notes: The values in parentheses are the ratios of increase in time and memory, respectively, as measured relative to the time and memory used by our S-PSM

Table 5.2: [16-layer structure] Processing CPU times / Residuals / Memory of S-PSM, ICCG, and CG for difference arrangements grid points.

Number of grid points			S-PSM			ICCG (EPS=1.0E-6)		ICCG (EPS=1.0E-10)			CG (EPS=1.0E-6)		CG (EPS=1.0E-10)		
matrix size (h*g)	h	g	CPU (sec)	Residual	Memory (MB)	CPU (sec)	Residual	CPU (sec)	Residual	Memory (MB)	CPU (sec)	Residual	CPU (sec)	Residual	Memory (MB)
2944	16	184	0.04 (1.0)	4.4E-16	8.0 (1.0)	0.07 (1.8)	9.9E-07	0.01 (2.6)	8.9E-11	6.3 (0.78)	0.30 (8.0)	8.8E-07	0.56 (15.0)	9.6E-11	5.9 (0.73)
10752	32	336	0.23 (1.0)	5.7E-15	17.1 (1.0)	0.45 (1.9)	6.4E-07	0.69 (3.0)	5.7E-11	8.7 (0.51)	2.80 (12.0)	9.5E-07	5.19 (22.3)	9.1E-11	7.0 (0.41)
40960	64	640	1.40 (1.0)	2.1E-14	56.9 (1.0)	3.45 (2.5)	8.8E-07	5.74 (4.1)	9.9E-11	13.2 (0.23)	28.7 (20.5)	9.9E-07	55.32 (39.5)	9.0E-11	9.2 (0.16)
159744	128	1248	8.48 (1.0)	1.4E-13	73.7 (1.0)	21.7 (2.6)	8.7E-07	38.6 (4.6)	9.9E-11	36.0 (0.49)	211.8 (25.0)	9.8E-07	447.6 (52.8)	9.5E-11	20.7 (0.28)
630784	256	2464	48.5 (1.0)	1.4E-12	124.4 (1.0)	147.6 (3.0)	9.4E-07	274.8 (5.7)	8.3E-11	126.3 (1.02)	1465.7 (30.2)	9.9E-07	3157.1 (65.1)	9.6E-11	65.9 (0.53)

Notes: The values in parentheses are the ratios of increase in time and memory, respectively, as measured relative to the time and memory used by our S-PSM

Table 5.3: [32-layer structure] Processing CPU times / Residuals / Memory of S-PSM, ICCG, and CG for difference arrangements grid points.

Number of grid points			S-PSM			ICCG (EPS=1.0E-6)		ICCG (EPS=1.0E-10)			CG (EPS=1.0E-6)		CG (EPS=1.0E-10)		
matrix size (h*g)	h	g	CPU (sec)	Residual	Memory (MB)	CPU (sec)	Residual	CPU (sec)	Residual	Memory (MB)	CPU (sec)	Residual	CPU (sec)	Residual	Memory (MB)
4736	16	296	0.08 (1.0)	3.1E-15	10.6 (1.0)	0.15 (2.05)	7.7E-07	0.22 (2.9)	7.2E-11	6.9 (0.65)	0.68 (9.1)	9.6E-07	1.26 (16.8)	8.2E-11	6.1 (0.58)
16896	32	528	0.41 (1.0)	8.2E-15	28.5 (1.0)	1.13 (2.75)	9.5E-07	1.76 (4.3)	8.2E-11	8.6 (0.30)	7.10 (17.2)	9.9E-07	13.87 (33.6)	9.8E-11	6.94 (0.24)
63488	64	992	2.65 (1.0)	3.9E-14	106.9 (1.0)	7.6 (2.85)	7.7E-07	12.5 (4.7)	8.3E-11	17.5 (0.16)	58.1 (21.9)	8.9E-07	120.1 (45.4)	9.3E-11	11.4 (0.11)
245760	128	1920	15.8 (1.0)	2.2E-13	142.8 (1.0)	46.2 (2.93)	9.9E-07	82.3 (5.2)	9.8E-11	52.5 (0.37)	446.1 (28.3)	9.4E-07	927.7 (58.9)	9.9E-07	28.9 (0.20)
966656	256	3776	93.4 (1.0)	2.1E-12	235.9 (1.0)	302.7 (3.25)	9.2E-07	596.0 (6.4)	9.9E-11	190.7 (0.81)	3036.7 (32.5)	9.9E-07	6814.9 (73.0)	9.9E-11	98.1 (0.42)

Notes: The values in parentheses are the ratios of increase in time and memory, respectively, as measured relative to the time and memory used by our S-PSM